Dissipativity-Based Synthesis of Distributed Control and Communication Topology Co-Design for AC Microgrids

Mohammad Javad Najafirad, Shirantha Welikala, Lei Wu, and Panos J. Antsaklis

Abstract—This paper presents a novel dissipativity-based framework for co-designing distributed controllers and communication topologies in AC microgrids (MGs). Unlike existing methods that treat control synthesis and topology design separately, we propose a unified approach that simultaneously optimizes both aspects to achieve voltage and frequency regulation and proportional power sharing among distributed generators (DGs). We formulate the closed-loop AC MG as a networked system where DGs, distribution lines, and loads are interconnected subsystems characterized by their dissipative properties. Each DG employs a hierarchical architecture combining local controllers for voltage regulation and distributed controllers for droop-free power sharing through normalized power consensus. By leveraging dissipativity theory, we establish necessary and sufficient conditions for subsystem passivity and cast the codesign problem as a convex linear matrix inequality (LMI) optimization, enabling efficient computation and guaranteed stability. Our framework systematically synthesizes sparse communication topologies while handling the coupled dq-frame dynamics and dual power flow objectives inherent to AC MGs. Simulation results on a representative AC MG demonstrate the effectiveness of the proposed approach in achieving accurate voltage regulation, frequency synchronization, and proportional power sharing.

Index Terms—AC Microgrid, Voltage Regulation, Distributed Control, Networked Systems, Dissipativity-Based Control, Topology Design.

I. INTRODUCTION

The integration of renewable energy sources into power systems has accelerated the development of microgrids (MGs) as a reliable solution for electric energy sustainability. AC MGs, in particular, have emerged as critical components of modern power infrastructure and provide enhanced flexibility to manage distributed generators (DGs), energy storage systems, and various load types within localized networks [1]. Nevertheless, the control architecture of AC MGs faces significant challenges to maintain voltage stability, frequency synchronization, and proportional power sharing among DGs, particularly in islanded operation where no utility grid support is available [2]. These challenges become more complex due to the inherent nature of AC systems, which must manage both active and reactive power flows while multiple DGs operate in parallel synchronization [3]. Recent advances in networked control theory and communication technologies have opened new avenues to

Mohammad Javad Najafirad, Shirantha Welikala, and Lei Wu are with the Department of Electrical and Computer Engineering, School of Engineering and Science, Stevens Institute of Technology, Hoboken, NJ 07030, {mnajafir, swelikal, lei.wu}@stevens.edu. Panos J. Antsaklis is with the Department of Electrical Engineering, University of Notre Dame, Notre Dame, IN 46556, pantsakl@nd.edu.

develop sophisticated control strategies that address these multifaceted challenges through coordinated operation rather than purely local control actions [4].

Traditional control strategies for AC MGs have evolved from centralized to decentralized and distributed approaches to address scalability and reliability concerns [5]. Centralized control offers precise coordination but suffers from single points of failure and communication bottlenecks, while fully decentralized methods sacrifice optimal performance for local autonomy [6]. Distributed control emerges as a balanced solution that enables DGs to coordinate through sparse communication networks while each unit maintains local control authority [7]. The challenge lies in the design of both the control algorithms and the communication topology to achieve desired performance objectives. Most existing distributed control methods assume predetermined communication structures that mirror the physical electrical connections, which may not offer optimal information exchange patterns [8]. Furthermore, the complex nature of AC systems requires careful consideration of both voltage magnitude and phase angle dynamics, as well as the coupled relationship between active and reactive power flows [9].

Dissipativity theory provides a powerful framework to analyze and design control systems for interconnected networks by characterizing subsystems through their energy exchange properties [10]. Unlike traditional Lyapunov methods that require detailed system models, dissipativity-based approaches need only input-output energy relationships, greatly simplifying the analysis of complex networked systems [11]. Recent applications to AC MGs have shown promise in addressing voltage stabilization and power quality issues through passivity-based methods, though most approaches still rely on predetermined control structures without considering communication optimization [12]. The compositional nature of dissipativity theory allows modular design where individual DG controllers can be synthesized independently while guaranteeing overall system stability, a critical feature for scalable AC MG architectures [9]. However, the extension to comprehensive AC system control presents unique challenges due to the coupling between voltage components in the dq reference frame, the inherent complexity of threephase power systems, and the need to manage both active and reactive power flows [13]. The ability to guarantee stability through compositional certification makes dissipativity particularly attractive for modular AC MG architectures.

Despite these theoretical advances, most existing distributed control methods for AC MGs treat controller design and communication topology as separate problems, potentially missing optimal solutions that arise from their joint consideration [14]. Current approaches typically assume fixed communication structures or require all-to-all information exchange, which becomes impractical as MG size increases [15]. Moreover, simultaneously achieving voltage regulation and proportional power sharing in AC systems requires careful coordination of both active and reactive power controllers, a challenge not fully addressed by existing methods [16]. The need for a systematic co-design framework that jointly optimizes control parameters and communication topology while guaranteeing stability through rigorous theoretical foundations motivates this work.

This paper presents a novel dissipativity-based control and communication topology co-design framework for AC MGs with the following contributions:

- 1) We formulate the AC MG control problem as a networked system where DGs and distribution lines are modeled as interconnected subsystems with specific dissipative properties.
- 2) We develop a unified LMI-based co-design methodology that simultaneously optimizes distributed controllers and communication topology for both active and reactive power sharing.
- 3) We establish necessary and sufficient conditions for subsystem passivity that ensure the feasibility of the global co-design problem.

This work builds upon the dissipativity-based framework established in [17] for DC MGs and the systematic codesign methodology developed in [18] for vehicular platoons, extending these concepts to address the unique challenges of AC MG control with coupled dq dynamics and dual power flow objectives.

II. PRELIMINARIES

Notations: Notations \mathbb{R} and \mathbb{N} respectively signify the sets of real and natural numbers. For any $N \in \mathbb{N}$, we define $\mathbb{N}_N \triangleq \{1, 2, ..., N\}$. An $n \times m$ block matrix A is denoted as $A=[A_{ij}]_{i\in\mathbb{N}_n,j\in\mathbb{N}_m}$. Either subscripts or superscripts are used for indexing purposes, e.g., $A_{ij} = A^{ij}$. $[A_{ij}]_{j \in \mathbb{N}_m}$ and $\operatorname{diag}([A_{ii}]_{i\in\mathbb{N}_n})$ respectively represent a block row matrix and a block diagonal matrix. 0 and I are the zero and identity matrices, with proper dimensions clear from the context. A symmetric positive definite (semi-definite) matrix $A \in \mathbb{R}^{n \times n}$ is denoted by A > 0 (A > 0). The symbol \star represents conjugate blocks inside block a symmetric matrices. $\mathcal{H}(A) \triangleq$ $A + A^{\top}$. $\mathbf{1}_{\{\cdot\}}$ is the indicator function.

A. Dissipativity

Consider a general non-linear dynamic system

$$\dot{x}(t) = f(x(t), u(t)),
y(t) = h(x(t), u(t)),$$
(1)

where $x(t) \in \mathbb{R}^n$, $u(t) \in \mathbb{R}^q$, $y(t) \in \mathbb{R}^m$, and $f: \mathbb{R}^n \times \mathbb{R}^q \to \mathbb{R}^q$ \mathbb{R}^n and $h: \mathbb{R}^n \times \mathbb{R}^q \to \mathbb{R}^m$ are continuously differentiable. The equilibrium points of (1) are such that there is a unique $u^* \in \mathbb{R}^q$ that meets $f(x^*, u^*) = 0$ for any $x^* \in \mathcal{X}$, where $\mathcal{X} \subset \mathbb{R}^n$ is the set of equilibrium states. Both u^* and $y^* \triangleq$ $h(x^*, u^*)$ are implicit functions of x^* .

The equilibrium-independent-dissipativity (EID) [19] is defined next to examine dissipativity of (1) without the explicit knowledge of its equilibrium points.

Definition 1: The system (1) is called EID under supply rate $s: \mathbb{R}^q \times \mathbb{R}^m \to \mathbb{R}$ if there is a continuously differentiable storage function $V:\mathbb{R}^n \times \mathcal{X} \to \mathbb{R}$ such that $V(x,x^*) > 0$ when $x \neq x^*$, $V(x^*,x^*) = 0$, and $\dot{V}(x,x^*) = \nabla_x V(x,x^*) f(x,u) \le s(u-u^*,y-y^*),$ for all $(x, x^*, u) \in \mathbb{R}^n \times \mathcal{X} \times \mathbb{R}^q$.

This EID property can be specialized based on the used supply rate s(.,.). The X-EID property, defined in the sequel, uses a quadratic supply rate determined by a coefficient matrix $X = X^{\top} \triangleq [X^{kl}]_{k,l \in \mathbb{N}_2} \in \mathbb{R}^{q+m}$ [20].

Definition 2: The system (1) is X-EID if it is EID under the quadratic supply rate:

$$s(u-u^*,y-y^*) \triangleq \begin{bmatrix} u-u^* \\ y-y^* \end{bmatrix}^\top \begin{bmatrix} X^{11} & X^{12} \\ X^{21} & X^{22} \end{bmatrix} \begin{bmatrix} u-u^* \\ y-y^* \end{bmatrix}.$$

 $s(u-u^*,y-y^*) \triangleq \begin{bmatrix} u-u^* \\ y-y^* \end{bmatrix}^\top \begin{bmatrix} X^{11} & X^{12} \\ X^{21} & X^{22} \end{bmatrix} \begin{bmatrix} u-u^* \\ y-y^* \end{bmatrix}.$ **Remark** 1: If the system (1) is X-EID with: $1) \ X = \begin{bmatrix} 0 & \frac{1}{2}\mathbf{I} \\ \frac{1}{2}\mathbf{I} & \mathbf{0} \end{bmatrix}, \text{ then it is passive;}$ $2) \ X = \begin{bmatrix} -\nu \mathbf{I} & \frac{1}{2}\mathbf{I} \\ \frac{1}{2}\mathbf{I} & -\rho \mathbf{I} \end{bmatrix}, \text{ then it is strictly passive } (\nu \text{ and } \rho \text{ are the input and output passivity indices } \mathbf{I} = \mathbf{I}$ input and output passivity indices, denoted as IF-OFP(ν , ρ)); 3) $X = \begin{bmatrix} \gamma^2 \mathbf{I} & \mathbf{0} \\ \mathbf{0} & -\mathbf{I} \end{bmatrix}$, then it is L_2 -stable (γ is the L_2 -gain, denoted as $L2G(\gamma)$;

in an equilibrium-independent manner (see also [21]).

If the system (1) is linear time-invariant (LTI), a necessary and sufficient condition for X-EID is provided in the following proposition as an LMI problem.

Proposition 1: [18] The LTI system

$$\dot{x}(t) = Ax(t) + Bu(t), \quad y(t) = Cx(t) + Du(t),$$

is X-EID if and only if there exists P > 0 such that

$$\begin{bmatrix} -\mathcal{H}(PA) + C^{\top}X^{22}C & -PB + C^{\top}X^{21} + C^{\top}X^{22}D \\ \star & X^{11} + \mathcal{H}(X^{12}D) + D^{\top}X^{22}D \end{bmatrix} \geq 0.$$

The following corollary considers a specific LTI system with a local controller (a setup useful later) and formulates an LMI problem for X-EID enforcing local controller synthesis.

Corollary 1: [18] The LTI system

$$\dot{x}(t) = (A + BL)x(t) + \eta(t), \quad y(t) = x(t),$$

is X-EID with $X^{22} < 0$ if and only if there exists P > 0and K such that

$$\begin{bmatrix} -(X^{22})^{-1} & P & 0\\ \star & -\mathcal{H}(AP+BK) & -\mathbf{I}+PX^{21}\\ \star & \star & X^{11} \end{bmatrix} \ge 0,$$

and $L = KP^{-1}$.

B. Networked Systems

Consider the networked system Σ that consists of dynamic subsystems $\Sigma_i, i \in \mathbb{N}_N$ and $\bar{\Sigma}_i, i \in \mathbb{N}_{\bar{N}}$ which are linked via a static interconnection matrix M, with the exogenous inputs $w(t) \in \mathbb{R}^r$ (e.g. disturbances) and interested outputs $z(t) \in \mathbb{R}^l$ (e.g. performance).

The dynamics of each subsystem Σ_i , $i \in \mathbb{N}_N$ are given by

$$\dot{x}_i(t) = f_i(x_i(t), u_i(t)),
y_i(t) = h_i(x_i(t), u_i(t)),$$
(2)

where $x_i(t) \in \mathbb{R}^{n_i}$, $u_i(t) \in \mathbb{R}^{q_i}$, $y_i(t) \in \mathbb{R}^{m_i}$. Similar to (1), each subsystem $\Sigma_i, i \in \mathbb{N}_N$ is considered to have a set $\mathcal{X}_i \subset \mathbb{R}^{n_i}$, where for every $x_i^* \in \mathcal{X}_i$, there exists a unique $u_i^* \in \mathbb{R}^{q_i}$ such that $f_i(x_i^*, u_i^*) = 0$, and both u_i^* and $y_i^* \triangleq h_i(x_i^*, u_i^*)$ are implicit function of x_i^* . Moreover, each subsystem $\Sigma_i, i \in \mathbb{N}_N$ is assumed to be X_i -EID, where $X_i \triangleq [X_i^{kl}]_{k,l \in \mathbb{N}_2}$. Regarding each subsystem $\Sigma_i, i \in \mathbb{N}_N$, we use similar assumptions and notations, but include a bar symbol to highlight that Σ_i is X_i -EID where $X_i \triangleq [X_i^{kl}]_{k,l \in \mathbb{N}_2}$.

Defining $u \triangleq [u_i^\top]_{i \in \mathbb{N}_N}^\top$, $y \triangleq [y_i^\top]_{i \in \mathbb{N}_N}^\top$, $\bar{u} \triangleq [\bar{u}_i^\top]_{i \in \mathbb{N}_{\bar{N}}}^\top$ and $\bar{y} \triangleq [y_i^\top]_{i \in \mathbb{N}_{\bar{N}}}^\top$, the interconnection matrix M and the corresponding interconnection relationship are given by

$$\begin{bmatrix} u \\ \bar{u} \\ z \end{bmatrix} = M \begin{bmatrix} y \\ \bar{y} \\ w \end{bmatrix} \equiv \begin{bmatrix} M_{uy} & M_{u\bar{y}} & M_{uw} \\ M_{\bar{u}y} & M_{\bar{u}\bar{y}} & M_{\bar{u}w} \\ M_{zy} & M_{z\bar{y}} & M_{zw} \end{bmatrix} \begin{bmatrix} y \\ \bar{y} \\ w \end{bmatrix}. \tag{3}$$

The following proposition exploits the X_i -EID and \bar{X}_i -EID properties of the subsystems $\Sigma_i, i \in \mathbb{N}_N$ and $\bar{\Sigma}_i, i \in \mathbb{N}_{\bar{N}}$ to formulate an LMI problem for synthesizing the interconnection matrix M (3), ensuring the networked system Σ is **Y**-EID for a prespecified **Y** under two mild assumptions [20].

Assumption 1: For the networked system Σ , the provided **Y**-EID specification is such that $\mathbf{Y}^{22} < 0$.

Remark 2: Based on Rm. 1, Assumption 1 holds if the networked system Σ must be either: (i) L2G(γ) or (ii) IF-OFP(ν, ρ) with some $\rho > 0$, i.e., L_2 -stable or passive, respectively. Therefore, Assumption 1 is mild since it is usually preferable to make the networked system Σ either L_2 -stable or passive.

Assumption 2: In the networked system Σ , each subsystem Σ_i is X_i -EID with $X_i^{11} > 0, \forall i \in \mathbb{N}_N$, and similarly, each subsystem $\bar{\Sigma}_i$ is \bar{X}_i -EID with $\bar{X}_i^{11} > 0, \forall i \in \mathbb{N}_{\bar{N}}$.

Remark 3: According to Rm. 1, Assumption 2 holds if a subsystem $\Sigma_i, i \in \mathbb{N}_N$ is either: (i) L2G(γ_i) or (ii) IF-OFP(ν_i, ρ_i) with $\nu_i < 0$ (i.e., L_2 -stable or non-passive). Since in passivity-based control, often the involved subsystems are non-passive (or can be treated as such), Assumption 2 is also mild.

Proposition 2: [20] Under Assumptions 1 and 2, the network system Σ can be made Y-EID (from w(t) to z(t)) by synthesizing the interconnection matrix M through solving the LMI problem:

Find: $L_{uy}, L_{u\bar{y}}, L_{uw}, L_{\bar{u}y}, L_{\bar{u}\bar{y}}, L_{\bar{u}w}, M_{zy}, M_{z\bar{y}}$, and M_{zw} , s.t.: $p_i \geq 0, \forall i \in \mathbb{N}_N, \quad \bar{p}_l \geq 0, \forall l \in \mathbb{N}_{\bar{N}}, \text{ and (5)},$

with $\begin{bmatrix} M_{uy} & M_{u\bar{y}} & M_{uw} \\ M_{\bar{u}y} & M_{u\bar{y}} & M_{\bar{u}w} \end{bmatrix} = \begin{bmatrix} \mathbf{X}_p^{11} & \mathbf{0} \\ \mathbf{0} & \bar{\mathbf{X}}_p^{11} \end{bmatrix}^{-1} \begin{bmatrix} L_{uy} & L_{u\bar{y}} & L_{uw} \\ L_{\bar{u}y} & L_{\bar{u}\bar{y}} & L_{\bar{u}w} \end{bmatrix}$, where $\mathbf{X}_p^{11} = \operatorname{diag}(\{p_iX_i^{11} : i \in \mathbb{N}_N\}), \ \bar{\mathbf{X}}_{\bar{p}}^{11} = \operatorname{diag}(\{\bar{p}_i\bar{X}_i^{11} : i \in \mathbb{N}_{\bar{N}}\}), \ \mathbf{X}^{12} \triangleq \operatorname{diag}((X_i^{11})^{-1}X_i^{12} : i \in \mathbb{N}_N), \ \mathbf{X}^{21} \triangleq (\mathbf{X}^{12})^{\top}, \ \bar{\mathbf{X}}^{12} \triangleq \operatorname{diag}((\bar{X}_i^{11})^{-1}\bar{X}_i^{12} : i \in \mathbb{N}_{\bar{N}}), \ \operatorname{and} \ \bar{\mathbf{X}}^{21} \triangleq (\bar{\mathbf{X}}^{12})^{\top}.$

III. SYSTEM MODELING

This section presents the dynamic modeling of the AC MG, which consists of multiple DGs, loads, and power distribution lines. Our modeling approach is motivated by [22], which demonstrates the effectiveness of passivity-based analysis for voltage and frequency stabilization in islanded AC MGs. Building upon their electrical modeling framework, we extend the analysis to include power flow relationships and distributed coordination mechanisms. We introduce both local voltage controllers and distributed power sharing controllers for the AC MG and represent the closed-loop AC MG as a networked system suitable for dissipativity-based analysis.

A. AC MG Topology

The physical interconnection topology of an AC MG is modeled as a directed connected graph $\mathcal{G}^p = (\mathcal{V}, \mathcal{E})$. \mathcal{V} is partitioned into two sets: $\mathcal{M} = \{1,...,N+M\}$ represents DGs $\mathcal{D} = \{1,...,N\}$ and loads $\mathcal{L} = \{N+1,...,N+M\}$ with $\mathcal{M} = \mathcal{D} \cup \mathcal{L}$, and $\mathcal{P} = \{N+M+1,...,N+M+L\}$ is the set of distribution lines. Individual DGs and loads are interfaced with the AC MG through a point of common coupling (PCC), see Fig. 1 for a representative AC MG diagram. The orientation of each edge represents the reference direction of positive currents, which is arbitrarily assigned. A line cannot have only in-neighbors or out-neighbors, as the current entering in a line must leave it. Indeed, each node in \mathcal{P} is always connected to two distinct nodes in \mathcal{M} through two directed edges. We define a matrix $\mathcal{B} \in \mathbb{R}^{(N+M) \times L}$, with DGs and loads along rows and lines along columns, as

$$\mathcal{B}_{kl} = \begin{cases} 1 & l \in \mathcal{E}_k^+ \\ -1 & l \in \mathcal{E}_k^- \end{cases}, \quad k \in \mathcal{M}, \ l \in \mathcal{P}, \qquad (6)$$

$$0 \quad \text{otherwise}$$

where $\mathcal{E}_k^+ = \{l \in \mathcal{V} : (k,l) \in \mathcal{E}\}$ denotes the set of out-neighbors, $\mathcal{E}_k^- = \{j \in \mathcal{V} : (j,k) \in \mathcal{E}\}$ the set of inneighbors, and $\mathcal{N}_k = \mathcal{E}_k^+ \cup \mathcal{E}_k^-$ the set of neighbors.

For analysis purposes in this paper, we define the following neighbor sets. For physical topology, each Σ_i^{DG} has a physical neighbor set $\mathcal{N}_i^P = \{l: \mathcal{B}_{il} \neq 0\}$ representing the distribution lines connected to Σ_m^{DG} . Similarly, each Σ_m^{load} has a physical neighbor set $\mathcal{N}_m^P = \{l: \mathcal{B}_{ml} \neq 0\}$ representing the distribution lines connected to Σ_m^{load} . Conversely, each distribution line Σ_i^{line} has a physical neighbor set $\mathcal{N}_l^P = \{k: \mathcal{B}_{kl} \neq 0\}$ representing the DGs and loads connected to Σ_i^{line} .

B. Dynamic Model of a DG

Each DG comprises a DC voltage source, a voltage source converter (VSC), and series RLC filter components. The $\{\Sigma_i^{DG}: i \in \mathbb{N}_N\}$ supplies power to local loads in

$$\begin{bmatrix} \mathbf{X}_{p}^{11} & \mathbf{0} & \mathbf{0} & L_{uy} & L_{u\bar{y}} & L_{uw} \\ \mathbf{0} & \bar{\mathbf{X}}_{\bar{p}}^{11} & \mathbf{0} & L_{\bar{u}y} & L_{\bar{u}\bar{y}} & L_{\bar{u}w} \\ \mathbf{0} & \mathbf{0} & -\mathbf{Y}^{22} & -\mathbf{Y}^{22}M_{zy} & -\mathbf{Y}^{22}M_{z\bar{y}} & \mathbf{Y}^{22}M_{zw} \\ L_{uy}^{\top} & L_{\bar{u}y}^{\top} & -M_{z\bar{y}}^{\top}\mathbf{Y}^{22} & -L_{uy}^{\top}\mathbf{X}^{12} - \mathbf{X}^{21}L_{uy} - \mathbf{X}_{\bar{p}}^{22} & -\mathbf{X}^{21}L_{u\bar{y}} - L_{\bar{u}\bar{y}}^{\top}\bar{\mathbf{X}}^{12} & -\mathbf{X}^{21}L_{uw} + M_{z\bar{y}}^{\top}\mathbf{Y}^{21} \\ L_{u\bar{y}}^{\top} & L_{\bar{u}\bar{y}}^{\top} & -M_{z\bar{y}}^{\top}\mathbf{Y}^{22} & -L_{u\bar{y}}^{\top}\mathbf{X}^{12} - \bar{\mathbf{X}}^{21}L_{\bar{u}y} & -(L_{\bar{u}\bar{y}}^{\top}\bar{\mathbf{X}}^{12} + \bar{\mathbf{X}}^{21}L_{\bar{u}\bar{y}} + \bar{\mathbf{X}}_{\bar{p}}^{22}) & -\bar{\mathbf{X}}^{21}L_{\bar{u}w} + M_{z\bar{y}}^{\top}\mathbf{Y}^{21} \\ L_{uw}^{\top} & L_{u\bar{w}}^{\top} & -M_{zw}^{\top}\mathbf{Y}^{22} & -L_{uw}^{\top}\mathbf{X}^{12} + \mathbf{Y}^{12}M_{zy} & -L_{\bar{u}w}^{\top}\bar{\mathbf{X}}^{12} + \mathbf{Y}^{12}M_{z\bar{y}} & M_{zw}^{\top}\mathbf{Y}^{21} + \mathbf{Y}^{12}M_{zw} + \mathbf{Y}^{11} \end{bmatrix} > 0$$

$$(5)$$

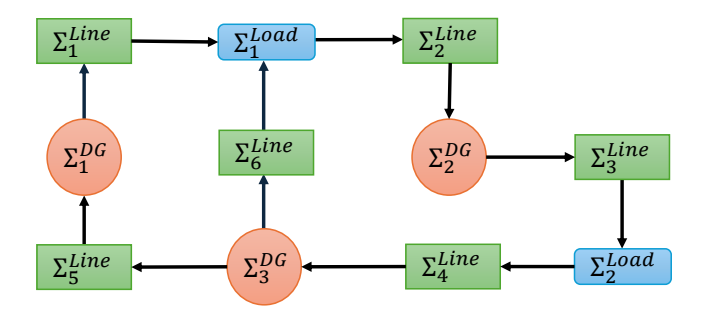


Fig. 1. A representative diagram of the AC MG network. The sets \mathcal{D} , \mathcal{L} , and ${\cal P}$ are represented as DGs, distribution lines and loads.

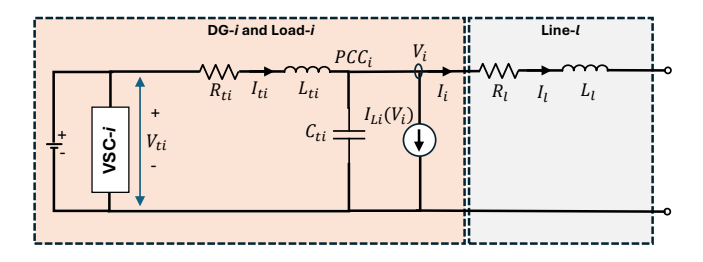


Fig. 2. Electrical scheme of DG i and distribution line l for AC MG.

its PCC_i while maintaining interconnection with other DG units through distribution lines $\{\Sigma_l^{line}: l \in \mathcal{E}_i\}$. Figure 2 illustrates the electrical schematic of Σ_i^{DG} , including the DG, local loads, and connected distribution line.

Motivated by the modeling approach in [22], we represent all three-phase electrical signals in a common direct and quadrature axis (dq) reference frame rotating at the nominal network frequency ω_0 . This representation enables systematic control design while maintaining the coupling between dq components. By applying Kirchhoff's current law (KCL) at PCC_i on the DG side, we obtain the following for Σ_i^{DG} :

$$C_{ti} \frac{dV_i^{dq}}{dt} = -C_{ti} j\omega_0 V_i^{dq} + I_{ti}^{dq} - I_{Li}^{dq} (V_i^{dq}) - I_i^{dq},$$

$$L_{ti} \frac{dI_{ti}^{dq}}{dt} = -V_i^{dq} - (R_{ti} + L_{ti} j\omega_0) I_{ti}^{dq} + V_{ti}^{dq},$$
(7)

where $V_i^{dq} = V_i^d + jV_i^q$, $I_{ti}^{dq} = I_{ti}^d + jI_{ti}^q$, and the net current injected into the AC MG by Σ_i^{DG} is given by: $I_i^{dq} = \sum_{l \in \mathcal{E}_i} \mathcal{B}_{il} I_l^{dq}. \tag{8}$

$$I_i^{dq} = \sum_{l \in \mathcal{E}_i} \mathcal{B}_{il} I_l^{dq}. \tag{8}$$

The $j\omega_0$ terms in (7) represent the cross-coupling between d and q components inherent in the rotating reference frame, where the $+j\omega_0$ term coupling in the voltage equation corresponds to the natural dynamics of AC quantities in the synchronously rotating frame, while the $-j\omega_0$ term in the current equation accounts for the inductance-based phase relationships.

In (7), the parameters R_{ti} , L_{ti} , and C_{ti} represent the internal resistance, inductance, and filter capacitance of Σ_i^{DG} , respectively. The state variables are selected as V_i^d , V_i^q (the dq-components of PCC_i voltage) and I_{ti}^d , I_{ti}^q (the the dq-components of filter current). The term $V_{ti}^{dq} = V_{ti}^d + \mathrm{j} V_{ti}^q$ represents the control input command applied at the VSC, $I_{Li}^{dq}=I_{Li}^d+\mathrm{j}I_{Li}^q$ denotes the local load current, and $I_i^{dq}=I_i^d+\mathrm{j}I_i^q$ represents the total current injection to the AC MG

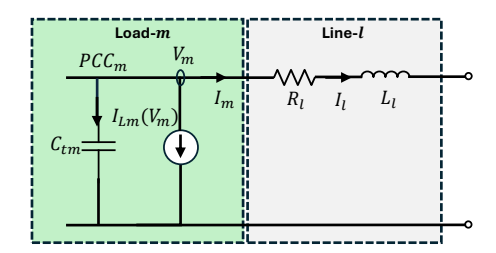


Fig. 3. Electrical scheme of ZIP load in AC MG.

by Σ_i^{DG} .

C. Line Power Flow Calculation

The active and reactive power injections to the AC MG by each Σ_i^{DG} are denoted respectively as P_i and Q_i , which can be calculated via V_i^{dq} (PCC_i voltage) and I_i^{dq} (total current injection (8)), as [23]:

$$P_{i} = V_{i}^{d} I_{i}^{d} + V_{i}^{q} I_{i}^{q},$$

$$Q_{i} = V_{i}^{q} I_{i}^{d} - V_{i}^{d} I_{i}^{q}.$$
(9)

This formulation provides direct calculation of power outputs without requiring explicit phase-angle tracking, thereby maintaining consistency with the single synchronously rotating reference frame. The calculated active and reactive power values serve as feedback signals for the distributed consensus-based control in Sec. IV-C, enabling proportional power sharing among DGs.

D. Load Model

The loads in the AC MG are modeled as a combination of constant impedance (Z), constant current (I), and constant power (P) components, commonly referred to as ZIP loads.

Each local load is connected at a DG terminal through its respective PCC. At Σ_i^{DG} , the local load current

$$I_{Li}^{dq} = I_{Li}^{Z} + I_{Li}^{I} + I_{Li}^{P} = Y_{Li}V_{i}^{dq} + \bar{I}_{Li}^{dq} + P_{Li}^{dq},$$
 (10)

where Y_{Li} represents the load admittance, \bar{I}_{Li}^{dq} denotes the constant current component, and P_{Li}^{dq} is the constant power component of the load.

On the other hand, the m-th global load $\Sigma_m^{Load},$ along with its connecting power lines (at PCC_m), is shown in Fig. 3. Similar to local loads, the total global load current comprises three components:

$$I_{Lm}^{dq} = I_{Lm}^{Z} + I_{Lm}^{I} + I_{Lm}^{P} = Y_{Lm}V_{m}^{dq} + \bar{I}_{Lm}^{dq} + P_{Lm}^{dq},$$
(11)

where Y_{Lm} represents the load admittance, \bar{I}_{Lm}^{dq} denotes the constant current component, and P_{Lm}^{dq} is the constant power component of the load.

We consider the dynamic effects of global loads, particularly those arising from load filter capacitance. By applying KCL at PCC_m , we obtain the dynamic model of the global load Σ_m^{Load} in dq frame as:

$$\frac{dV_{m}^{dq}}{dt} = -\mathrm{j}\omega_{0}V_{m}^{dq} - \frac{1}{C_{tm}}\left(Y_{Lm}V_{m}^{dq} + \bar{I}_{Lm}^{dq} + P_{Lm}^{dq}\right) - \frac{I_{m}^{dq}}{C_{tm}},\tag{12}$$

where I_m^{dq} is the net current injection from connected distribution lines. The net current injected into the AC MG by Σ_m^{Load} is given by:

$$I_m^{dq} = \sum_{l \in \mathcal{E}_m} \mathcal{B}_{ml} I_l^{dq}. \tag{13}$$

The state space representation of Σ_i^{load} is:

$$\dot{\tilde{x}}_m(t) = \check{A}_m \check{x}_m(t) + \check{B}_m \check{u}_m(t) + \check{B}_m \check{d}_m(t), \tag{14}$$

where the state vector is $\check{x}_m = \begin{bmatrix} V_m^d & V_m^q \end{bmatrix}^{\top}$, the exogenous input is $\check{d}_m = \begin{bmatrix} \bar{I}_{Lm}^d & \bar{I}_{Lm}^q \end{bmatrix}^{\top}$ (which represents the constant current load component under the common assumption $P_{Lm}^{dq} = 0$), and the coupling input is $\check{u}_m = \begin{bmatrix} I_m^d & I_m^q \end{bmatrix}^{\top}$. The system matrices \check{A}_m and \check{B}_m in (14) respectively are

$$\check{A}_{m} \triangleq \begin{bmatrix} -\frac{Y_{Lm}}{C_{tm}} & \omega_{0} \\ -\omega_{0} & -\frac{Y_{Lm}}{C_{tm}} \end{bmatrix}, \text{ and } \check{B}_{m} \triangleq \begin{bmatrix} -\frac{1}{C_{tm}} & 0 \\ 0 & -\frac{1}{C_{tm}} \end{bmatrix}.$$

$$\tag{15}$$

E. Distribution Line Model

Each distribution line is represented using π -equivalent circuit model, where the line capacitances are lumped with the DG filter capacitances at the connection points. Following the modeling approach in [22], the distribution line Σ_l^{line} is modeled as an RL circuit with resistance R_l and inductance L_l . By applying Kirchhoff's voltage law (KVL) to Σ_l^{line} we obtain its dynamic model in the dq reference frame as:

$$\frac{dI_l^{dq}}{dt} = -\left(\frac{R_l}{L_l} + j\omega_0\right)I_l^{dq} + \frac{1}{L_l}\sum_{i \in \mathcal{N}^P} \mathcal{B}_{il}V_i^{dq}, \quad (16)$$

where $I_l^{dq}=I_l^d+\mathrm{j}I_l^q$ represents the current flowing through Σ_l^{line} . The voltage difference across the line (which excites the line dynamics, also called the coupling input) is determined by the PCC voltages of the connected DGs/loads.

The distribution line dynamics capture the inductive and resistive effects in the dq frame while maintaining the coupling between d and q components through the ω_0 terms, which represent the natural dynamics of AC quantities in the synchronously rotating reference frame.

Separating the real and imaginary components, the state space representation of Σ_l^{line} can be obtained as:

$$\dot{\bar{x}}_l(t) = \bar{A}_l \bar{x}_l(t) + \bar{B}_l \bar{u}_l(t), \tag{17}$$

where the state vector is $\bar{x}_l = \begin{bmatrix} I_l^d & I_l^q \end{bmatrix}^\top$, and the coupling input is

$$\bar{u}_{l} = \sum_{k \in \mathcal{N}_{l}^{P}} \mathcal{B}_{kl} \begin{bmatrix} V_{k}^{d} & V_{k}^{q} \end{bmatrix}^{\top}.$$
 (18)

The system matrices in (17) are:

$$\bar{A}_l \triangleq \begin{bmatrix} -\frac{R_l}{L_l} & \omega_0 \\ -\omega_0 & -\frac{R_l}{L_l} \end{bmatrix}, \quad \bar{B}_l \triangleq \begin{bmatrix} \frac{1}{L_l} & 0 \\ 0 & \frac{1}{L_l} \end{bmatrix}. \tag{19}$$

IV. PROPOSED CONTROLLERS

The control architecture for the AC MG employs a hierarchical structure with three layers: local steady-state controllers for equilibrium point adjustment, local feedback controllers for voltage regulation at each Σ_i^{DG} , and distributed controllers for coordinated power sharing among DGs via communication networks. The local steady-state controllers ensure a proper operating equilibrium point for

the AC MG, mitigating steady-state errors; the local feedback controllers ensure fast voltage tracking at each PCC; the distributed controllers ensure proportional power sharing by coordinating frequency references without centralized coordination.

A. Local Feedback Controllers

Each DG is equipped with local feedback controllers that enable tracking a given PCC voltage reference. To achieve precise voltage tracking, each $\Sigma_i^{DG}, i \in \mathbb{N}_N$ is augmented with an integral voltage tracking error state v_i^{dq} , of which the dynamics are:

$$\dot{v}_i^{dq}(t) = e_i^{dq}(t) = V_i^{dq} - V_{i ref}^{dq}, \tag{20}$$

where $v_i^{dq}=v_i^d+\mathrm{j}v_i^q$ represents the dq components of the integral voltage tracking error, and $V_{i,ref}^{dq}=V_{i,ref}^d+\mathrm{j}V_{i,ref}^q$ is a prespecified voltage reference.

Consequently, each Σ_i^{DG} is equipped with a PI-structured local feedback controller $u_{iL}(t)$ that uses only voltage measurements and integral states:

$$u_{iL}(t) \triangleq K_i^P \begin{bmatrix} e_i^d(t) \\ e_i^q(t) \end{bmatrix} + K_i^I \int_0^t \begin{bmatrix} e_i^d(\tau) \\ e_i^q(\tau) \end{bmatrix} d\tau$$

$$= K_{i0}x_i(t) - K_i^P \begin{bmatrix} V_{i,ref}^d \\ V_{i,ref}^q \end{bmatrix}, \tag{21}$$

where $x_i(t)$ denotes the augmented state vector of Σ_i^{DG} , defined as

$$x_i \triangleq \begin{bmatrix} V_i^d & V_i^q & I_{ti}^d & I_{ti}^q & v_i^d & v_i^q & \tilde{\omega}_i \end{bmatrix}^\top, \quad (22)$$

(the augmented local state component $\tilde{\omega}_i$ will be formally introduced in the sequel, but it is not required here for local controllers), $K_{i0} = \begin{bmatrix} K_i^P & \mathbf{0}_{2\times 2} & K_i^I & \mathbf{0}_{2\times 1} \end{bmatrix} \in \mathbb{R}^{2\times 7}$ is the local controller gain, and K_i^P and K_i^I are respectively the proportional and integral gain matrices of the local PI controllers.

Essentially, the local control input component $u_{iL}(t)$ of the total control input $u_i^V(t) \triangleq \begin{bmatrix} V_{ti}^d(t) & V_{ti}^q(t) \end{bmatrix}^\top$ at the VSC of Σ_i^{DG} is given by:

$$u_{iL}(t) = K_i^P \begin{bmatrix} V_i^d - V_{i,ref}^d \\ V_i^q - V_{i,ref}^q \end{bmatrix} + K_i^I \begin{bmatrix} v_i^d \\ v_i^q \end{bmatrix}.$$
 (23)

This local control architecture provides feedback from all augmented states to both d-axis and q-axis voltage control commands, enabling cross-coupling between d and q control channels when necessary for stability and performance.

B. Distributed Controllers for Frequency Synchronization

In islanded AC MG operation, each Σ_i^{DG} must generate a local frequency reference $\omega_i(t)$ for proper dq-frame transformation and system synchronization. The phase angle $\theta_i(t)$ required for the Park transformation is obtained through:

$$\theta_i(t) = \int_0^t \omega_i(\tau) d\tau. \tag{24}$$

To maintain frequency coherence while preserving droopfree power-sharing characteristics, we incorporate frequency dynamics via normalized power consensus [24]. However, directly implementing an algebraic relationship

$$\omega_i(t) = \omega_0 + u_i^{\Omega}(t),$$

with a distributed consensus control input

$$u_i^{\Omega}(t) = \sum_{j \in \mathcal{N}_i^C} K_{ij}^{\Omega} (P_{n,i}(t) - P_{n,j}(t)),$$
 (25)

(where $P_{n,i}(t) = P_i(t)/P_i^{\rm max}$ represents normalized active power injection from Σ_i^{DG}) would create an implicit system unsuitable for state-space analysis. Therefore, we model the frequency dynamics using a first-order filter that captures realistic measurement, communication, and actuation delays:

$$\tau_i \frac{d\omega_i(t)}{dt} = -\omega_i(t) + \omega_0 + u_i^{\Omega}(t), \qquad (26)$$

where $\tau_i > 0$ is a small time constant representing the combined effect of sensing, communication, and control delays in the frequency control loop. To obtain frequency error dynamics, we define $\tilde{\omega}_i = \omega_i - \omega_0$, which yields:

$$\tau_i \frac{d\tilde{\omega}_i(t)}{dt} = -\tilde{\omega}_i + u_i^{\Omega}(t). \tag{27}$$

The used distributed consensus control input $u_i^\Omega(t)$ ensures that frequency deviations are directly proportional to normalized power imbalances among communicating DGs. When all DGs reach normalized power consensus, the system frequency converges to the nominal value ω_0 , achieving both proportional power sharing and frequency synchronization objectives without compromising the droop-free operation principle. More details on the used distributed controllers are discussed in the following subsection.

C. Distributed Controllers for Proportional Power Sharing

While the local controllers ensure voltage regulation, they do not address proportional power sharing among DGs. To achieve proportional power sharing, we use distributed global controllers that leverage communication networks (droopfree) to eliminate the need for centralized coordination.

The distributed control strategy employs consensus-based algorithms to achieve proportional sharing of active and reactive power among DGs. For each Σ_i^{DG} , the distributed control laws are:

$$u_{i}^{P}(t) = \sum_{j \in \mathcal{N}_{i}^{C}} K_{ij}^{P} (P_{i,n}(t) - P_{j,n}(t)),$$

$$u_{i}^{Q}(t) = \sum_{j \in \mathcal{N}_{i}^{C}} K_{ij}^{Q} (Q_{i,n}(t) - Q_{j,n}(t)),$$
(28)

where K_{ij}^P and K_{ij}^Q are the active and reactive power sharing distributed controller gains, and $P_{i,n}(t) = P_i(t)/P_i^{\max}$ and $Q_{i,n}(t) = Q_i(t)/Q_i^{\max}$ are the normalized active and reactive power values with P_i^{\max} and Q_i^{\max} being the maximum power ratings of Σ_i^{DG} . Recall that the active and reactive power measurements $P_i(t)$ and $Q_i(t)$ at each DG Σ_i^{DG} can be obtained via (9).

The overall VSC control input $u_i^V(t) \triangleq \begin{bmatrix} V_{ti}^d(t) & V_{ti}^q(t) \end{bmatrix}^\top$ combines local steady-state controllers, local feedback controllers and global distributed controllers:

$$u_i^V(t) \triangleq \begin{bmatrix} V_{ti}^d(t) \\ V_{ti}^q(t) \end{bmatrix} = u_{iS} + u_{iL}(t) + u_{iG}(t),$$
 (29)

where $u_{iG}(t) = \begin{bmatrix} u_i^P(t) & u_i^Q(t) \end{bmatrix}^{\top}$ represents the distributed controller (28), $u_{iL}(t)$ is the local controller (21), and u_{iS}

is the steady-state controller (to be designed in the sequel). It is worth noting that we can restate (29) in dq frame as

$$u_i^{Vdq}(t) \triangleq V_{ti}^{dq}(t) = u_{iS}^{dq} + u_{iL}^{dq}(t) + u_{iC}^{dq}(t).$$
 (30)

This droop-free approach eliminates the traditional tradeoff between voltage regulation and power sharing accuracy by directly coordinating through communication rather than relying on local droop characteristics.

D. Closed-Loop Dynamics of the AC MG

By combining (7), (20) and (27), the overall dynamics of Σ_i^{DG} , $i \in \mathbb{N}_N$ can be written as:

$$\frac{dV_i^{dq}}{dt} = -i(\omega_0 + \tilde{\omega}_i)V_i^{dq} + \frac{I_{ti}^{dq}}{C_{ti}} - \frac{I_{Li}^{dq}}{C_{ti}} - \frac{I_i^{dq}}{C_{ti}} + w_{vi}^{dq}(t),$$
(31a)

$$\frac{dI_{ti}^{dq}}{dt} = -\frac{V_i^{dq}}{L_{ti}} - \left(\frac{R_{ti}}{L_{ti}} + i(\omega_0 + \tilde{\omega}_i)\right) I_{ti}^{dq} + \frac{u_i^{Vdq}}{L_{ti}} + w_{ci}^{dq}(t),$$
(31b)

$$\frac{dv_i^{dq}}{dt} = V_i^{dq} - V_{i,ref}^{dq},\tag{31c}$$

$$\frac{d\tilde{\omega}_i}{dt} = -\frac{1}{\tau_i}\tilde{\omega}_i + \frac{1}{\tau_i}u_i^{\Omega},\tag{31d}$$

where the terms I_i^{dq} , I_{Li}^{dq} , u_i^{Vdq} , and u_i^{Ω} can all be substituted from (8), (10), (30) and (25), respectively, and $w_{vi}^{dq}(t)$ and w_{ci}^{dq} are unknown zero-mean disturbances (accounting for model uncertainities and external impacts). Using the commonly adopted assumption $P_{Li}^{dq} = 0$ (for (10)), the dynamics of Σ_i^{DG} (31) can be written in compact state-space form as: $\dot{x}_i(t) = A_i x_i(t) + B_i u_i(t) + E_i d_i(t) + F_i \xi_i(t) + g_i(x_i(t))$,

$$\dot{x}_i(t) = A_i x_i(t) + B_i u_i(t) + E_i d_i(t) + F_i \xi_i(t) + g_i(x_i(t)).$$
(32)

where $x_i(t)$ is the state vector as defined in (22), $u_i(t) \triangleq \begin{bmatrix} u_i^V(t) & u_i^{\Omega}(t) \end{bmatrix}^{\top}$ is the total control input, $d_i(t)$ is the exogenous input (disturbance) defined as:

$$d_i(t) \triangleq \bar{w}_i + w_i(t),\tag{33}$$

with $\bar{w}_i \triangleq \begin{bmatrix} -\bar{I}_{Li}^d & -\bar{I}_{Li}^q & 0 & 0 & -V_{i,ref}^d & -V_{i,ref}^q & 0 \end{bmatrix}^\top$ representing the known fixed (mean) disturbance and $w_i(t) = \begin{bmatrix} w_{vi}^d(t) & w_{vi}^q(t) & w_{ci}^d(t) & w_{ci}^q(t) & 0 & 0 & 0 \end{bmatrix}^\top$ representing the unknown zero-mean disturbance, $\xi_i(t) \triangleq \begin{bmatrix} I_i^d & I_i^q \end{bmatrix}^\top$ is the distribution line coupling input (recall $I_i^{dq} = \sum_{l \in \mathcal{E}_i} \mathcal{B}_{il} I_l^{dq}(t)$), and

$$g_i(x_i(t)) \triangleq \begin{bmatrix} -\tilde{\omega}_i V_i^q & -\tilde{\omega}_i V_i^d & -\tilde{\omega}_i I_{ti}^q & -\tilde{\omega}_i I_{ti}^d & 0 & 0 & 0 \end{bmatrix}^\top,$$
(34)

captures the nonlinear coupling terms.

In (32), the system matrix A_i , control input matrix B_i , disturbance input matrix E_i , and distribution line coupling

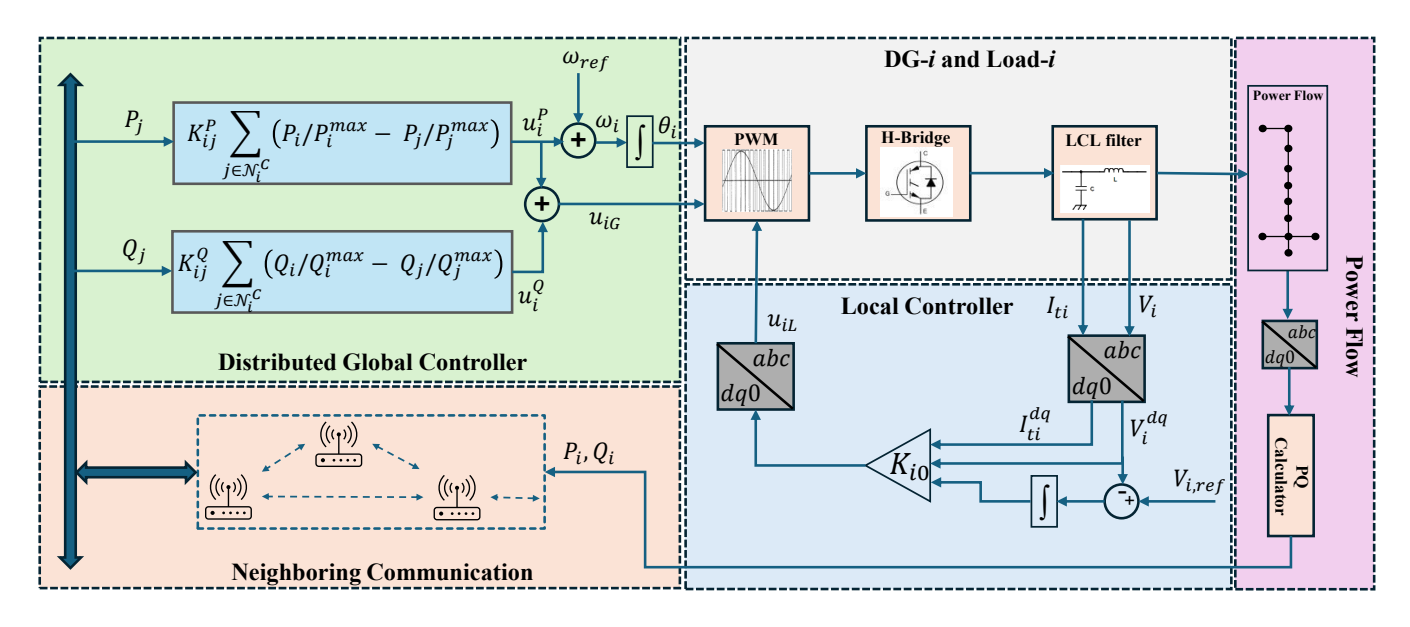


Fig. 4. Hierarchical control architecture combining local and distributed controllers through physical and communication interconnections.

matrix F_i are given respectively by:

E. Networked System Representation

This subsection formulates the closed-loop AC MG as a networked system by establishing the interconnection relationships among DGs, lines, and loads through a static interconnection matrix. We analyze each subsystem type systematically to identify its coupling mechanisms, then construct the aggregate interconnection relationship. Figure 5 illustrates the identified overall networked system representation of the AC MG.

1) **DG Subsystems**: Note that each DG control input $u_i(t)$ in (32) can be expressed as

$$u_i(t) = \begin{bmatrix} u_i^V(t) \\ u_i^{\Omega}(t) \end{bmatrix} = \begin{bmatrix} \mathbf{I}_{2\times 2} \\ \mathbf{0}_{1\times 2} \end{bmatrix} (u_{iS} + u_{iL}(t)) + u_i^D(t),$$

where u_{iS} is the steady-state controller, $u_{iL}(t)$ is the local feedback controller that takes the form (21):

$$u_{iL}(t) = K_{i0}x_i(t) - K_i^P \begin{bmatrix} V_{i,ref}^d \\ V_{i,ref}^q \end{bmatrix},$$

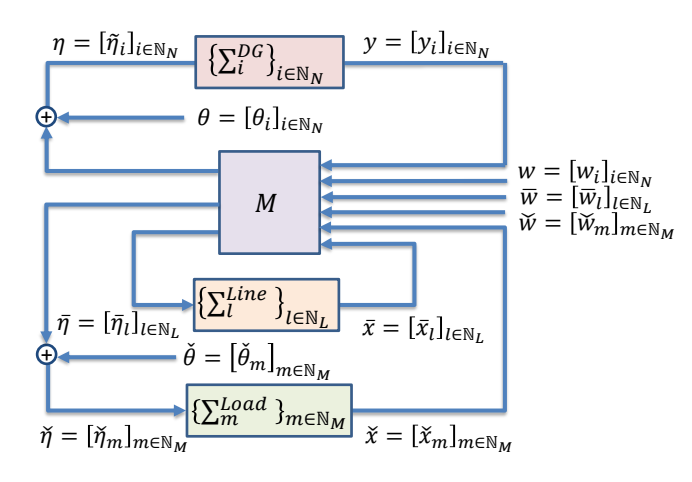


Fig. 5. Networked system representation showing interconnections between DGs, lines, and loads AC MG.

and $u_i^D(t)$ is the global distributed controller that takes the form (by combining (25), (28)):

$$u_{i}^{D}(t) \triangleq \begin{bmatrix} u_{i}^{G}(t) \\ u_{i}^{Q}(t) \end{bmatrix} = \begin{bmatrix} u_{i}^{P}(t) \\ u_{i}^{Q}(t) \\ u_{i}^{Q}(t) \end{bmatrix}$$

$$= \sum_{j \in \mathcal{N}_{i}^{C}} \underbrace{\begin{bmatrix} K_{ij}^{P} & \mathbf{0} \\ \mathbf{0} & K_{ij}^{Q} \\ K_{ij}^{Q} & \mathbf{0} \end{bmatrix}}_{\triangleq K_{ij}} \begin{bmatrix} P_{i,n}(t) - P_{j,n}(t) \\ Q_{i,n}(t) - Q_{j,n}(t) \end{bmatrix}$$

$$= \sum_{j \in \tilde{\mathcal{N}}_{i}^{C}} \hat{K}_{ij} \begin{bmatrix} P_{j}(t) \\ Q_{j}(t) \end{bmatrix}, \tag{36}$$

where we define $\bar{\mathcal{N}}_i^C \triangleq \mathcal{N}_i^C \cup \{i\}$, and

$$\hat{K}_{ij} \triangleq \begin{cases} -\bar{K}_{ij} \begin{bmatrix} P_j^{\text{max}} & \mathbf{0} \\ 0 & Q_j^{\text{max}} \end{bmatrix}^{-1}, & j \in \mathcal{N}_i^C, \\ \sum_{j \in \mathcal{N}_i^C} \bar{K}_{ij} \begin{bmatrix} P_i^{\text{max}} & \mathbf{0} \\ 0 & Q_i^{\text{max}} \end{bmatrix}^{-1}, & j = i. \end{cases}$$
(37)

It is worth noting that, when designing \hat{K}_{ij} blocks, to uniquely obtain the corresponding distributed controller gain matrices K_{ij}^P, K_{ij}^Q , and K_{ij}^Ω , we have to embed two structural constraints: (i) each off-diagonal \hat{K}_{ij} block (i.e., $j \neq i$) should be structured similarly to the corresponding \bar{K}_{ij} block (i.e., with three inner **0** blocks, see (36)); and (ii) each diagonal \hat{K}_{ij} block (i.e., \hat{K}_{ii}) should satisfy

$$\hat{K}_{ii} = -\sum_{j \in \mathcal{N}_i^C} \hat{K}_{ij} \begin{bmatrix} P_j^{\text{max}} & \mathbf{0} \\ 0 & Q_j^{\text{max}} \end{bmatrix} \begin{bmatrix} P_i^{\text{max}} & \mathbf{0} \\ 0 & Q_i^{\text{max}} \end{bmatrix}^{-1}.$$
(38)

Applying this $u_i(t)$ form in (32), we can obtain the closed-loop dynamics of each DG subsystem Σ_i^{DG} , $i \in \mathbb{N}_N$ as:

$$\dot{x}_i(t) = \hat{A}_i x_i(t) + \hat{B}_i \eta_i(t) + g_i(x_i(t)) + \theta_i, \tag{39}$$

where $\hat{A}_i \triangleq A_i + \bar{B}_i K_{i0}$, $\bar{B}_i \triangleq B_i \begin{bmatrix} \mathbf{I}_{2\times 2} & \mathbf{0}_{2\times 1} \end{bmatrix}^{\top}$, and $\hat{B}_i \triangleq \begin{bmatrix} B_i & F_i & E_i \end{bmatrix}$. In (39), $g_i(x_i)$ represents the frequency coupling nonlinearity defined in (34), θ_i represents the effective steady-state input that takes the form:

$$\theta_i \triangleq \bar{B}_i(u_{iS} - K_i^P \begin{bmatrix} V_{i,ref}^d \\ V_{i,ref}^q \end{bmatrix}) + E_i \bar{w}_i,$$

and $\eta_i(t)$ represents the effective control input, defined as

$$\eta_i(t) \triangleq \begin{bmatrix} u_i^D(t) \\ \xi_i(t) \\ w_i(t) \end{bmatrix}, \tag{40}$$

where $u_i^D(t)$ is the distributed control input (through the communication topology), $\xi_i(t)$ is the distribution line coupling input that takes the form:

$$\xi_i = \begin{bmatrix} I_i^d \\ I_i^q \end{bmatrix} = \sum_{l \in \mathcal{E}_i} \mathcal{B}_{il} \begin{bmatrix} I_l^d \\ I_l^q \end{bmatrix} = \sum_{l \in \mathcal{E}_i} \bar{C}_{il} \bar{x}_l,$$

where $\bar{C}_{il} \triangleq \mathcal{B}_{il}\mathbf{I}_2$, and $w_i(t)$ represents the unknown zero-mean disturbances from (33).

Since the injected active and reactive power (from power flow equations (9)) and PCC voltage of each DG impact other elements in the AC MG, we define an output vector y_i for each Σ_i^{DG} as:

$$y_i \triangleq \begin{bmatrix} V_i^d & V_i^q & P_i & Q_i \end{bmatrix}^\top = h_i(x_i, \eta_i).$$
 (41)

The first two components V_i^d and V_i^q of the output y_i are the first two components of the DG state x_i in (39). These DG output components affect the physically connected line dynamics (17) via (18), as they determine the line inputs as:

$$\bar{u}_l = \sum_{k \in \mathcal{N}^P} \mathcal{B}_{kl} \begin{bmatrix} V_k^d \\ V_k^q \end{bmatrix} = \sum_{k \in \mathcal{N}^P} C_{lk} y_k,$$

where $C_{lk} \triangleq \mathcal{B}_{kl} \begin{bmatrix} \mathbf{I}_2 & \mathbf{0}_{2\times 2} \end{bmatrix} = \begin{bmatrix} \mathcal{B}_{kl} \mathbf{I}_2 & \mathbf{0}_{2\times 2} \end{bmatrix}$. On the other hand, the last two components P_i and Q_i of the output y_i can be computed via (9) using DG state components

 V_i^d , V_i^q and DG input component ξ_i in (39). These DG output components affect the dynamics of neighboring DGs (39) via (36), as they determine the distributed control input as

$$u_i^D = \sum_{j \in \bar{\mathcal{N}}_i^C} \hat{K}_{ij} \begin{bmatrix} P_j \\ Q_j \end{bmatrix} = \sum_{j \in \bar{\mathcal{N}}_i^C} \tilde{K}_{ij} y_j,$$

where $K_{ij} \triangleq \hat{K}_{ij} \begin{bmatrix} \mathbf{0}_{2 \times 2} & \mathbf{I}_2 \end{bmatrix} = \begin{bmatrix} \mathbf{0}_{3 \times 2} & \hat{K}_{ij} \end{bmatrix}$.

2) Line Subsystems: Each distribution line subsystem Σ_l^{Line} , $l \in \mathbb{N}_L$ follows the dynamics from (17):

$$\dot{\bar{x}}_l(t) = \bar{A}_l \bar{x}_l(t) + \hat{\bar{B}}_l \bar{\eta}_l(t), \tag{42}$$

where

$$\hat{\bar{B}}_l \triangleq \begin{bmatrix} \bar{B}_l & \bar{B}_l & \bar{E}_l \end{bmatrix},\tag{43}$$

with \bar{B}_l as defined in (19), and $\bar{E}_l \triangleq (1/L_l)\mathbf{I}_2$. In (42), $\bar{\eta}_l$ represents the effective input (driven mainly by the applied voltage difference by the connected DGs and Loads) that takes the form:

$$\bar{\eta}_{l}(t) = \begin{bmatrix} \sum_{k \in \mathcal{N}_{l}^{P}} C_{lk} y_{k}(t) \\ \sum_{m \in \mathcal{N}_{l}^{P}} \check{C}_{lm} \check{x}_{m}(t) \\ \bar{w}_{l}(t) \end{bmatrix}, \tag{44}$$

where

$$C_{lk} \triangleq \mathcal{B}_{kl} \begin{bmatrix} \mathbf{I}_2 & \mathbf{0}_{2\times 2} \end{bmatrix} = \begin{bmatrix} \mathcal{B}_{kl} \mathbf{I}_2 & \mathbf{0}_{2\times 2} \end{bmatrix},$$
 (45)

$$\check{C}_{lm} \triangleq \mathcal{B}_{ml} \mathbf{I}_2, \tag{46}$$

and $\bar{w}_l(t)$ represents an unknown zero-mean disturbance (added on to (17)) to account for model uncertainties.

3) Load Subsystems: Each load subsystem $\Sigma_m^{Load}, m \in \mathbb{N}_M$ follows dynamics from (14):

$$\dot{\dot{x}}_m(t) = \check{A}_m \check{x}_m(t) + \dot{\check{B}}_m \check{\eta}_m(t) + \check{\theta}_m(t), \tag{47}$$

where

$$\hat{B}_m \triangleq \begin{bmatrix} \check{B}_m & \check{E}_m \end{bmatrix}, \tag{48}$$

with \check{B}_m as defined in (15) and $\check{E}_m \triangleq \check{B}_m$. In (47), $\check{\theta}_m$ represents the steady-state input that takes the form $\check{\theta}_m \triangleq \check{B}_m \check{d}_m$, $\check{\eta}_m(t)$ represents the effective input (driven mainly by currents injected from connected lines) that takes the form:

$$\check{\eta}_m(t) \triangleq \left[\begin{array}{c} \sum_{l \in \mathcal{E}_i} \check{C}_{ml} \bar{x}_l(t) \\ \check{w}_m(t) \end{array} \right], \tag{49}$$

where

$$\dot{\tilde{C}}_{ml} \triangleq \mathcal{B}_{ml} \mathbf{I}_2, \tag{50}$$

and $\check{w}_m(t)$ represents an unknown zero-mean disturbance (added on to (14)) to account for model uncertainties.

4) Networked System Representation: We now construct the networked system representation by vectorizing the identified subsystem dynamics. For DG subsystems, vectorizing (39), (41) and (40) yields:

$$\begin{cases} \dot{x}(t) = \hat{A}x(t) + \hat{B}\eta(t) + G(x(t)) + \theta, \\ y(t) = H(x(t), \eta(t)), \\ \eta(t) = Ky(t) + \bar{C}\bar{x}(t) + Ew(t), \end{cases}$$
(51)

where we define the vectors: $x \triangleq \begin{bmatrix} x_i^\top \end{bmatrix}_{i \in \mathbb{N}_N}^\top, \eta \triangleq \begin{bmatrix} \eta_i^\top \end{bmatrix}_{i \in \mathbb{N}_N}^\top, \theta \triangleq \begin{bmatrix} \theta_i^\top \end{bmatrix}_{i \in \mathbb{N}_N}^\top, y \triangleq \begin{bmatrix} y_i^\top \end{bmatrix}_{i \in \mathbb{N}_N}^\top, \bar{x} \triangleq \begin{bmatrix} \bar{x}_l^\top \end{bmatrix}_{l \in \mathbb{N}_L}^\top, w \triangleq \begin{bmatrix} w_i^\top \end{bmatrix}_{i \in \mathbb{N}_N}^\top, \text{ the matrices: } \hat{A} \triangleq \text{diag}(\begin{bmatrix} \hat{A}_i \end{bmatrix}_{i \in \mathbb{N}_N}), \ \hat{B} \triangleq \frac{1}{N} = \frac{1}{N} =$

$$\begin{split} \operatorname{diag}(\left[\hat{B}_{i}\right]_{i\in\mathbb{N}_{N}}), \\ K &\triangleq \begin{bmatrix} K_{ij} \\ \mathbf{0} \\ \mathbf{0} \end{bmatrix}_{i,j\in\mathbb{N}_{N}}, \quad \bar{C} \triangleq \begin{bmatrix} \mathbf{0} \\ \bar{C}_{il} \\ \mathbf{0} \end{bmatrix}_{i\in\mathbb{N}_{N},l\in\mathbb{N}_{L}}, \\ E &\triangleq \operatorname{diag}(\begin{bmatrix} \mathbf{0} \\ \mathbf{0} \\ \mathbf{I} \end{bmatrix}_{i\in\mathbb{N}_{N}}), \end{split}$$

and the vector spaces:

$$\begin{split} G(x) &\triangleq \left[g_i^\top(x_i)\right]_{i \in \mathbb{N}_N}^\top, \quad H(x) \triangleq \left[h_i^\top(x_i, \eta_i)\right]_{i \in \mathbb{N}_N}^\top. \end{split}$$
 For line subsystems, vectorizing (42) and (44) yields:

$$\begin{cases} \dot{\bar{x}}(t) = \bar{A}\bar{x}(t) + \bar{B}\bar{\eta}(t), \\ \bar{\eta}(t) = Cx(t) + \check{C}\check{x}(t) + \bar{E}\bar{w}(t), \end{cases}$$
(52)

where we define the vectors $\bar{\eta} \triangleq \begin{bmatrix} \bar{\eta}_l^\top \end{bmatrix}_{l \in \mathbb{N}_L}^\top$, $\check{x} \triangleq \begin{bmatrix} \check{x}_m^\top \end{bmatrix}_{m \in \mathbb{N}_M}^\top$, $\bar{w} \triangleq \left[\bar{w}_l^\top\right]_{l \in \mathbb{N}_L}^\top, \text{ and the matrices } \bar{A} \triangleq \operatorname{diag}(\left[\bar{A}_l\right]_{l \in \mathbb{N}_L}), \; \bar{B} \triangleq$ $\operatorname{diag}(\left[\bar{B}_l\right]_{l\in\mathbb{N}_L}),$

$$C \triangleq \begin{bmatrix} C_{lk} \\ \mathbf{0} \\ \mathbf{0} \end{bmatrix}_{l \in \mathbb{N}_L, k \in \mathbb{N}_N}, \quad \check{C} \triangleq \begin{bmatrix} \mathbf{0} \\ \check{C}_{lm} \\ \mathbf{0} \end{bmatrix}_{l \in \mathbb{N}_L, m \in \mathbb{N}_M},$$

$$\bar{E} \triangleq \operatorname{diag}(\begin{bmatrix} \mathbf{0} \\ \mathbf{0} \\ \mathbf{I} \end{bmatrix}_{l \in \mathbb{N}_L}).$$

For load subsystems, vectorizing (47) and (49) yields:

$$\begin{cases} \dot{\dot{x}}(t) = \check{A}\check{x}(t) + \dot{\hat{B}}\check{\eta}(t) + \check{\theta}, \\ \check{\eta}(t) = \bar{\check{C}}\bar{x}(t) + \check{E}\check{w}(t), \end{cases}$$
(53)

where we define the vectors $\check{\eta} \triangleq [\check{\eta}_m^\top]_{m \in \mathbb{N}_M}, \ \check{w} \triangleq$ $\begin{bmatrix} \check{w}_m^{\intercal} \end{bmatrix}_{m \in \mathbb{N}_M}^{\intercal}$, and $\check{\theta} \triangleq \begin{bmatrix} \check{\theta}_m^{\intercal} \end{bmatrix}_{m \in \mathbb{N}_M}^{\intercal}$, and the matrices: $\check{A} \triangleq \operatorname{diag}(\begin{bmatrix} \check{A}_m \end{bmatrix}_{m \in \mathbb{N}_M})$, $\hat{B} \triangleq \operatorname{diag}(\begin{bmatrix} \hat{B}_m \end{bmatrix}_{m \in \mathbb{N}_M})$,

$$\bar{\check{C}} = \begin{bmatrix} \bar{\check{C}}_{ml} \\ \mathbf{0} \end{bmatrix}_{m \in \mathbb{N}_M, l \in \mathbb{N}_L}, \quad \check{E} = \operatorname{diag}(\begin{bmatrix} \mathbf{0} \\ \mathbf{I} \end{bmatrix}_{m \in \mathbb{N}_M}).$$

The interconnection relationship among DGs (51), Lines (52) and Loads (53) now can be identified as:

$$\begin{bmatrix} \eta \\ \bar{\eta} \\ \check{\eta} \end{bmatrix} = \underbrace{\begin{bmatrix} K & \bar{C} & \mathbf{0} & E & \mathbf{0} & \mathbf{0} \\ C & \mathbf{0} & \check{C} & \mathbf{0} & \bar{E} & \mathbf{0} \\ \mathbf{0} & \check{C} & \mathbf{0} & \mathbf{0} & \mathbf{0} & \check{E} \end{bmatrix}}_{\triangleq M} \begin{bmatrix} y \\ \bar{x} \\ \check{x} \\ w \\ \bar{w} \\ \check{w} \end{bmatrix}, \qquad (54)$$

where M is the interconnection matrix.

*** Revised up to this....

V. NETWORKED SYSTEM ERROR DYNAMICS

This section analyzes the equilibrium points of the closedloop AC MG system and derives the error dynamics formulation suitable for dissipativity-based analysis. The equilibrium analysis establishes conditions under which voltage regulation, frequency synchronization, and proportional power sharing objectives are simultaneously achieved at steady

state. We then formulate the error dynamics by defining deviations from these equilibrium states, which enables us to analyze the system's stability and performance properties using the dissipativity framework developed in Sec. II.

A. Equilibrium Analysis and Error Variable Definitions

To analyze the stability properties when the networked system is perturbed from equilibrium, we define error variables as deviations from constant equilibrium states. For the DG, line, and load subsystems, the error variables are defined as:

$$\tilde{V}_i^{dq} \triangleq V_i^{dq} - V_{i ref}^{dq}, \tag{55a}$$

$$\tilde{I}_{ti}^{dq} \triangleq I_{ti}^{dq} - I_{tEi}^{dq},$$

$$\tilde{v}_{i}^{dq} \triangleq v_{i}^{dq} - v_{Ei}^{dq} = v_{i}^{dq},$$
(55b)

$$\tilde{v}_i^{dq} \triangleq v_i^{dq} - v_{Ei}^{dq} = v_i^{dq}, \tag{55c}$$

$$\tilde{\omega}_i \triangleq \tilde{\omega}_i - \tilde{\omega}_{Ei} = \tilde{\omega}_i, \tag{55d}$$

$$\tilde{I}_{l}^{dq} \triangleq I_{l}^{dq} - I_{El}^{dq}, \tag{55e}$$

$$\tilde{V}_m^{dq} \triangleq V_m^{dq} - V_{Em}^{dq},\tag{55f}$$

where $v_{Ei}^{dq}=0$ and $\tilde{\omega}_{Ei}=0$ at equilibrium due to the integral action and frequency synchronization objectives.

The equilibrium point is constant in time, determined solely by fixed reference signals and system parameters. Therefore, the time derivatives of all equilibrium states are

$$\dot{x}_{Ei} = 0$$
, $\dot{\bar{x}}_{El} = 0$, $\dot{\bar{x}}_{Em} = 0$.

Since the error states satisfy $\tilde{x}_i = x_i - x_{Ei}$, $\tilde{\bar{x}}_l = \bar{x}_l - \bar{x}_{El}$, and $\tilde{\check{x}}_m = \check{x}_m - \check{x}_{Em}$, their time derivatives are:

$$\begin{split} \dot{\ddot{x}}_i &= \dot{x}_i - \dot{x}_{Ei} = x_i, \\ \dot{\ddot{\ddot{x}}}_l &= \dot{\ddot{x}}_l - \dot{\ddot{x}}_{El} = \ddot{x}_l, \\ \dot{\ddot{\ddot{x}}}_m &= \dot{\ddot{x}}_m - \dot{\ddot{x}}_{Em} = \check{x}_m. \end{split}$$

This means that error dynamics can be derived by substituting error variables into the closed-loop dynamics equations (39), (42), and (47), and eliminating the constant equilibrium terms.

We substitute $x_i = \tilde{x}_i + x_{Ei}$ and $\eta_i = \tilde{\eta}_i + \eta_{iE}$ into the closed-loop DG dynamics (39) yields:

$$\dot{\tilde{x}}_i = \hat{A}_i(\tilde{x}_i + x_{Ei}) + \hat{B}_i(\tilde{\eta}_i + \eta_{iE}) + g_i(\tilde{x}_i + x_{Ei}) + \theta_i.$$

The frequency coupling nonlinearity defined in (34) has the structure $g_i(\tilde{x}_i + x_{Ei}) = g_i(\tilde{x}_i) + g_i(x_{Ei})$. At equilibrium, the frequency deviation is zero ($\tilde{\omega}_{Ei} = 0$), which implies $g_i(x_{Ei}) = 0$. Expanding the above equation and grouping

$$\dot{\tilde{x}}_i = \hat{A}_i \tilde{x}_i + \hat{B}_i \tilde{\eta}_i + g_i(\tilde{x}_i) + (\hat{A}_i x_{Ei} + \hat{B}_i \eta_{iE} + \theta_i),$$

wherea we enforce:

$$\hat{A}_i x_{Ei} + \hat{B}_i \eta_{iE} + \theta_i = 0. \tag{56}$$

This condition ensures that when the system is at equilibrium, all state derivatives are zero. The equilibrium is designed such that the frequency coupling nonlinearity and the distributed control vanish, and the steady-state offset θ_i balances the system dynamics.

Substituting the error variables defined in (55a)-(55d) into the closed-loop DG dynamics (39), the DG error dynamics become:

$$\dot{\tilde{x}}_i = \hat{A}_i \tilde{x}_i + \hat{B}_i \tilde{\eta}_i + g_i(\tilde{x}_i), \tag{57}$$

where \hat{A}_i and \hat{B}_i are defined in (39), $\tilde{\eta}_i$ represents the effective error augmented input, and $g_i(\tilde{x}_i)$ is the frequency coupling nonlinearity depending only on error states.

The error augmented input is defined as:

$$\tilde{\eta}_i \triangleq \eta_i - \eta_{iE},\tag{58}$$

where η_{iE} is the equilibrium augmented input. Since the disturbances w_i are zero-mean, we have $w_{iE}=0$ at equilibrium. From (40), the augmented error input takes the form:

$$\tilde{\eta}_{i}(t) = \begin{bmatrix} \sum_{j \in \mathcal{N}_{i}^{C}} \tilde{K}_{ij} \tilde{y}_{j}(t) \\ \sum_{l \in \mathcal{E}_{i}} \bar{C}_{il} \tilde{x}_{l}(t) \\ w_{i}(t) \end{bmatrix}.$$
 (59)

The frequency coupling nonlinearity, which depends only on error states, is:

$$g_i(\tilde{x}_i) \triangleq \begin{bmatrix} -\tilde{\omega}_i V_i^q & -\tilde{\omega}_i V_i^d & -\tilde{\omega}_i I_{ti}^q & -\tilde{\omega}_i I_{ti}^d & 0 & 0 & 0 \end{bmatrix}^\top.$$
(60)

The power measurements that derive the distributed control are linearized around the equilibrium operating point. Using the error variables, the active and reactive power deviations are approximated as:

$$\tilde{P}_{i} \triangleq P_{i} - P_{Ei} \approx V_{Ei}^{d} \tilde{I}_{i}^{d} + I_{Ei}^{d} \tilde{V}_{i}^{d} + V_{Ei}^{q} \tilde{I}_{i}^{q} + I_{Ei}^{q} \tilde{V}_{i}^{q},
\tilde{Q}_{i} \triangleq Q_{i} - Q_{Ei} \approx V_{Ei}^{q} \tilde{I}_{i}^{d} - V_{Ei}^{d} \tilde{I}_{i}^{q} + \tilde{V}_{i}^{q} I_{Ei}^{d} - \tilde{V}_{i}^{d} I_{Ei}^{q}.$$
(61)

The DG output y_i from (41) couples DG states to line states through the power flow calculations. Linearizing the bilinear products around equilibrium states $(V_{iq}^{dq}, I_{iq}^{dq})$ yields:

$$\tilde{y}_i = C_i^y \tilde{x}_i + D_i^y \tilde{\eta}_i, \tag{62}$$

where the linearized output and feedthrough matrices are:

We further define $C^y \triangleq \operatorname{diag}(\left[C_i^y\right]_{i \in \mathbb{N}_N})$ and $D^y \triangleq \operatorname{diag}(\left[D_{il}^y\right]_{i \in \mathbb{N}_N, l \in \mathbb{N}_L})$.

Similarly, for distribution line subsystems, substituting error variables into (42) yields:

$$\dot{\tilde{x}}_l = \bar{A}_l \tilde{x}_l + \hat{B}_l \tilde{\eta}_l, \tag{64}$$

where \bar{A}_l and \hat{B}_l are defined in (43), and \bar{w}_l are zero-mean disturbances with equilibrium value zero. The error line input is given by:

$$\tilde{\tilde{\eta}}_{l} = \begin{bmatrix} \sum_{k \in \mathcal{N}_{l}^{P} \cap \mathcal{D}} C_{lk} \tilde{y}_{k} \\ \sum_{m \in \mathcal{N}_{l}^{P} \cap \mathcal{L}} \check{C}_{lm} \tilde{x}_{m} \\ \bar{w}_{l} \end{bmatrix},$$
(65)

where C_{lk} and \check{C}_{lm} are defined in (45) and (46), respectively. For load subsystems, substituting error variables into (47) yields:

$$\dot{\tilde{x}}_m = \check{A}_m \tilde{x}_m + \hat{B}_m \tilde{\dot{\eta}}_m, \tag{66}$$

where \check{A}_m and \check{B}_m are defined in (48), and \check{w}_m is a zero-mean disturbance with an equilibrium value of zero. The error load input is:

$$\tilde{\check{\eta}}_{m} = \begin{bmatrix} \sum_{l \in \mathcal{E}_{m}} \bar{\check{C}}_{ml} \tilde{\bar{x}}_{l} \\ \check{w}_{m} \end{bmatrix}, \tag{67}$$

where $\bar{\check{C}}_{ml}$ is defined in (50).

To ensure dissipativity of this networked error system, we further define the performance outputs of each DG error subsystem $\tilde{\Sigma}_i^{DG}$, $i \in \mathbb{N}_N$ as:

$$z_i(t) \triangleq H_i \tilde{y}_i(t),$$
 (68)

where H_i can be selected as $H_i \triangleq \mathbf{I}_4, \forall i \in \mathbb{N}_N$. Similarly, for each line error subsystem $\tilde{\Sigma}_l^{Line}, l \in \mathbb{N}_L$, the performance output is:

$$\bar{z}_l(t) \triangleq \bar{H}_l \tilde{\bar{x}}_l(t),$$
 (69)

where $\bar{H}_l = \mathbf{I}_2$. For each load error subsystem $\tilde{\Sigma}_m^{Load}, m \in \mathbb{N}_M$, the performance output is:

$$\dot{z}_m(t) = \check{H}_m \tilde{\check{x}}_m(t), \tag{70}$$

where $\check{H}_m = \mathbf{I}_2$.

Vectorizing these performance outputs across all subsystems yields:

$$z = H\tilde{y}, \quad \bar{z} = \bar{H}\tilde{\bar{x}}, \quad \check{z} = \check{H}\tilde{\check{x}},$$
 (71)

where $H=\operatorname{diag}(\left[H_i\right]_{i\in\mathbb{N}_N}),\ \bar{H}=\operatorname{diag}(\left[\bar{H}_l\right]_{l\in\mathbb{N}_L}),$ and $\check{H}=\operatorname{diag}(\left[\check{H}_m\right]_{m\in\mathbb{N}_M}).$

To represent the networked error system dynamics in a compact form, we consolidate the performance outputs and disturbance input vectors as:

$$z_c \triangleq \begin{bmatrix} z & \bar{z} & \check{z} \end{bmatrix}^\top, \quad w_c \triangleq \begin{bmatrix} w & \bar{w} & \check{w} \end{bmatrix}^\top.$$
 (72)

The consolidated disturbance vector w_c affects the networked error dynamics of the DG error subsystems, line error subsystems, and load error subsystems through consolidated disturbance input matrices, which are defined as:

$$E_c \triangleq \begin{bmatrix} E & \mathbf{0} & \mathbf{0} \end{bmatrix}, \quad \bar{E}_c \triangleq \begin{bmatrix} \mathbf{0} & \bar{E} & \mathbf{0} \end{bmatrix}, \quad \check{E}_c \triangleq \begin{bmatrix} \mathbf{0} & \mathbf{0} & \check{E} \end{bmatrix},$$
(73)

where $E = \operatorname{diag}(\left[E_i\right]_{i \in \mathbb{N}_N})$, $\bar{E} = \operatorname{diag}(\left[\bar{E}_l\right]_{l \in \mathbb{N}_L})$, $\check{E} = \operatorname{diag}(\left[\check{E}_m\right]_{m \in \mathbb{N}_M})$. Analogously, the dependence of consolidated performance outputs on the networked error system states is described via consolidated performance matrices:

$$H_c \triangleq \begin{bmatrix} H & \mathbf{0} & \mathbf{0} \end{bmatrix}^{\top}, \ \bar{H}_c \triangleq \begin{bmatrix} \mathbf{0} & \bar{H} & \mathbf{0} \end{bmatrix}^{\top}, \ \check{H}_c \triangleq \begin{bmatrix} \mathbf{0} & \mathbf{0} & \check{H} \end{bmatrix}^{\top}.$$

Vectorizing the error dynamics in (57), (64), and (66) across all subsystems, the consolidated error dynamics are:

$$\begin{cases} \dot{\tilde{x}} = \hat{A}\tilde{x} + \hat{B}\tilde{\eta} + G(\tilde{x}), \\ \dot{\tilde{x}} = \bar{A}\tilde{x} + \hat{B}\tilde{\tilde{\eta}}, \\ \dot{\tilde{x}} = \tilde{A}\tilde{x} + \hat{B}\tilde{\tilde{\eta}}, \end{cases}$$
(75)

where $\tilde{x} \triangleq \left[\tilde{x}_i\right]_{i \in \mathbb{N}_N}$, $\tilde{\tilde{x}} \triangleq \left[\tilde{\tilde{x}}_l\right]_{l \in \mathbb{N}_L}$, and $\tilde{\tilde{x}} \triangleq \left[\tilde{\tilde{x}}_m\right]_{m \in \mathbb{N}_M}$.

The system matrices are defined as $\hat{A} \triangleq \operatorname{diag}(\left[A_i + B_i K_{i0}\right]_{i \in \mathbb{N}_N}), \ G(\tilde{x}) \triangleq \operatorname{diag}(\left[g_i(\tilde{x}_i)\right]_{i \in \mathbb{N}_N}), \ \bar{A} \triangleq \operatorname{diag}(\left[\bar{A}_l\right]_{l \in \mathbb{N}_L}), \ \operatorname{and} \ \check{A} \triangleq \operatorname{diag}(\left[A_m\right]_{m \in \mathbb{N}_M}).$

With these definitions and the derived error subsystem dynamics (57), (64), and (66), the closed-loop error dynamics of AC MG can be modeled as a networked error system as illustrated in Fig. 6. The interconnection relationship among error subsystems, disturbance inputs, and performance outputs is described by:

$$\begin{bmatrix} \tilde{u} & \tilde{\tilde{u}} & \tilde{u} & z_c \end{bmatrix}^{\top} = \tilde{M} \begin{bmatrix} \tilde{y} & \tilde{\tilde{x}} & \tilde{\tilde{x}} & w_c \end{bmatrix}^{\top}, \quad (76)$$

where the error interconnection matrix \tilde{M} takes the form:

$$\tilde{M} \triangleq \begin{bmatrix} \tilde{K} & \bar{C} & \mathbf{0} & E_c \\ C & \mathbf{0} & \check{C} & \bar{E}_c \\ \mathbf{0} & \bar{C} & \mathbf{0} & \check{E}_c \\ H_c & \bar{H}_c & \check{H}_c & \mathbf{0} \end{bmatrix}, \tag{77}$$

with $\tilde{K} = \left[\tilde{K}_{ij}\right]_{i,j\in\mathbb{N}_N}$.

B. Equilibrium Point Analysis of the AC MG

Lemma 1: If neglecting the zero-mean unknown disturbances, i.e., $w_i(t) = 0, \forall i \in \mathbb{N}_N, \ \bar{w}_l(t) = 0, \forall l \in \mathbb{N}_L,$ and $\check{w}_m(t) = 0, \forall m \in \mathbb{N}_M,$ then for a given reference voltage vector V_r , constant current load vector \bar{I}_{Li} and \bar{I}_{Lm} , and under the normalized power sharing objectives (28), there exists a unique equilibrium point for the AC MG characterized by:

$$V_E^{dq} = V_r, (78a)$$

$$\tilde{\omega}_E = \mathbf{0},\tag{78b}$$

$$I_{El}^{dq} = (Z_l^{dq})^{-1} \mathcal{B}_D^{\top} V_E^{dq} + (Z_l^{dq})^{-1} \mathcal{B}_L^{\top} V_{mE}^{dq}, \tag{78c}$$

$$V_{mE}^{dq} = -(Y_m^{dq})^{-1}(\bar{I}_{Lm}^{dq} + \mathcal{B}_L I_{El}^{dq}), \tag{78d}$$

$$I_{tE}^{dq} = (Z_{ti}^{dq})^{-1} (u_E^{dq} - V_E^{dq}), \tag{78e}$$

$$u_E^{dq} = V_r + Z_{ti}^{dq} (\Omega_0 C_{ti} V_r + \bar{I}_L + \mathcal{B}_D I_{El}^{dq}), \tag{78f}$$

where we define the equilibrium state vectors $V_E^{dq} \triangleq \begin{bmatrix} V_{Ei}^{dq} \end{bmatrix}_{i \in \mathbb{N}_N}^{\mathsf{T}} \in \mathbb{R}^{2N}$ (DG voltages with $V_{Ei}^{dq} = V_{i,ref}^{dq}$), $I_{tE}^{dq} \triangleq \begin{bmatrix} I_{tEi}^{dq} \end{bmatrix}_{i \in \mathbb{N}_N}^{\mathsf{T}} \in \mathbb{R}^{2N}$ (DG filter currents), $\tilde{\omega}_E \triangleq \begin{bmatrix} \tilde{\omega}_{Ei} \end{bmatrix}_{i \in \mathbb{N}_N}^{\mathsf{T}} \in \mathbb{R}^{2N}$ (line currents), $V_{mE}^{dq} \triangleq \begin{bmatrix} V_{mE}^{dq} \end{bmatrix}_{m \in \mathbb{N}_M}^{\mathsf{T}} \in \mathbb{R}^{2M}$ (load voltages), and $V_E^{dq} \triangleq \begin{bmatrix} V_{Ei}^{dq} \end{bmatrix}_{i \in \mathbb{N}_N}^{\mathsf{T}} \in \mathbb{R}^{2N}$ (equilibrium control inputs).

The incidence matrix $\mathcal{B} \in \mathbb{R}^{(N+M) \times L}$ defined in (6) is partitioned as $\mathcal{B} = \begin{bmatrix} \mathcal{B}_D^\top & \mathcal{B}_L^\top \end{bmatrix}^\top$, where $\mathcal{B}_D \in R^{N \times L}$ and $\mathcal{B}_L \in \mathbb{R}^{M \times L}$. The complex impedance and admittance matrices are $Z_l^{dq} \triangleq R_l + \Omega_{0l}L_l$, $Z_{ti}^{dq} \triangleq R_{ti} + \Omega_0L_{ti}$, and $Y_m^{dq} \triangleq Y_{Lm} + \Omega_{0m}C_{tm}$, with $\Omega_{0l} \triangleq \operatorname{diag}(\left[i\omega_0\mathbf{I}_2\right]_{l \in \mathbb{N}_L})$, $\Omega_0 \triangleq \operatorname{diag}(\left[i\omega_0\mathbf{I}_2\right]_{i \in \mathbb{N}_N})$, and $\Omega_{0m} \triangleq \operatorname{diag}(\left[i\omega_0\mathbf{I}_2\right]_{m \in \mathbb{N}_M})$. The system parameter matrices are $C_{ti} \triangleq \operatorname{diag}(\left[C_{ti}\right]_{i \in \mathbb{N}_N})$, $L_{ti} \triangleq \operatorname{diag}(\left[L_{ti}\right]_{i \in \mathbb{N}_N})$, $R_{ti} \triangleq \operatorname{diag}(\left[R_{ti}\right]_{i \in \mathbb{N}_N})$, $Y_L \triangleq \operatorname{diag}(\left[Y_{Li}\right]_{i \in \mathbb{N}_N})$, $R_l \triangleq \operatorname{diag}(\left[R_l\right]_{l \in \mathbb{N}_L})$, $L_l \triangleq \operatorname{diag}(\left[L_l\right]_{l \in \mathbb{N}_L})$, $C_{tm} \triangleq \operatorname{diag}(\left[C_{tm}\right]_{m \in \mathbb{N}_M})$, $Y_{Lm} \triangleq \operatorname{diag}(\left[Y_{Lm}\right]_{m \in \mathbb{N}_M})$, $\bar{I}_L \triangleq \operatorname{diag}(\left[\bar{I}_{Li}^{dq}\right]_{i \in \mathbb{N}_N}^\top) \in \mathbb{R}^{2N}$, and $\bar{I}_{Lm} \triangleq \left[\bar{I}_{Lm}^{dq}\right]_{m \in \mathbb{N}_M}^\top \in \mathbb{R}^{2M}$.

Proof: The equilibrium state of the closed-loop Σ_i^{DG}

dynamics (31) satisfies:

$$(A_i + B_i K_{i0}) x_{Ei} + g_i (x_{Ei}) + \theta_i + B_i u_{Di} + F_i \xi_{Ei} + E_i \bar{w}_i = 0,$$
 (79) where $x_{Ei} \triangleq \begin{bmatrix} V_{Ei}^d & V_{Ei}^q & I_{tEi}^d & I_{tEi}^q & v_{Ei}^d & v_{Ei}^q & \tilde{\omega}_{Ei} \end{bmatrix}^\top$ represents the equilibrium state components of Σ_i^{DG} , and A_{Ei} and $\xi_{Ei} = \begin{bmatrix} \sum_{l \in \mathcal{E}_i} \mathcal{B}_{il} I_{El}^{dq} \end{bmatrix}$ represent the distribution line coupling at equilibrium.

Since under the zero disturbance assumption the normalized power sharing control law (28) requires $P_{n,Ei} = P_{n,Ej}$ and $Q_{n,Ei} = Q_{n,Ej}$ for all communicating pairs, the distributed control input vanishes at equilibrium: $u_i^D = \left[u_{Ei}^P, u_{Ei}^Q\right] = 0$. Furthermore, the frequency deviation is zero at equilibrium ($\tilde{\omega}_{Ei} = 0$), implying $g_i(x_{Ei}) = 0$ from the definition in (34).

From the voltage equation of (79) with $\dot{V}_i^{dq} = 0$:

$$-i\omega_0 V_{Ei}^{dq} + \frac{1}{C_{ti}} I_{tEi}^{dq} - \frac{1}{C_{ti}} \bar{I}_{Li}^{dq} - \frac{1}{C_{ti}} \sum_{l \in \mathcal{E}_i} \mathcal{B}_{il} I_{El}^{dq} = 0.$$
 (80)

From the filter current equation of (79) with $\dot{I}_{ti}^{dq} = 0$:

$$-\frac{1}{L_{ti}}V_{Ei}^{dq} - \left(\frac{R_{ti}}{L_{ti}} + i\omega_0\right)I_{tEi}^{dq} + \frac{1}{L_{ti}}u_{Ei}^{dq} = 0.$$
 (81)

Rearranging (81) to solve for the equilibrium control input:

$$u_{Ei}^{dq} = V_{Ei}^{dq} + (R_{ti} + i\omega_0 L_{ti}) I_{tEi}^{dq}.$$
 (82)

Using the complex impedance notation $Z_{ti} \triangleq R_{ti} + i\omega_0 L_{ti}$:

$$u_{Ei}^{dq} = V_{Ei}^{dq} + Z_{ti}^{dq} L_{tEi}^{dq}. (83)$$

From the integral error equation of (79) with $\dot{v}_i^{dq} = 0$:

$$V_{Ei}^{dq} = V_{i,ref}^{dq}. (84)$$

From the frequency equation of (79) with $\dot{\tilde{\omega}}_i = 0$:

$$\tilde{\omega}_{Ei} = u_{Ei}^P. \tag{85}$$

However, at equilibrium, the normalized power sharing objective from (28) requires:

$$u_{Ei}^{P} = K_{ij}^{P} \sum_{j \in \mathcal{N}_{i}^{C}} (P_{n,Ei}(t) - P_{n,Ej}(t)) = 0,$$
 (86)

which implies $\tilde{\omega}_{Ei} = 0$ or $\omega_{Ei} = \omega_0$. This establishes (78b).

From (81), rearranging:

$$\left(\frac{R_{ti}}{L_{ti}} + i\omega_0\right)I_{tEi}^{dq} = \frac{1}{L_{ti}}u_{Ei}^{dq} - \frac{1}{L_{ti}}V_{Ei}^{dq}.$$
 (87)

Multiplying both sides by L_{ti} :

$$(R_{ti} + i\omega_0 L_{ti}) I_{tEi}^{dq} = u_{Ei}^{dq} - V_{Ei}^{dq}.$$

Using the complex impedance notation $Z_{ti}^{dq} \triangleq R_{ti} + i\omega_0 L_{ti}$:

$$I_{tEi}^{dq} = (Z_{ti}^{dq})^{-1} (u_{Ei}^{dq} - V_{Ei}^{dq}).$$

Substituting (84):

$$I_{tEi}^{dq} = (Z_{ti}^{dq})^{-1} (u_{Ei}^{dq} - V_{i\,ref}^{dq}). \tag{88}$$

Vectorizing equation (88) for all DGs $i \in \mathbb{N}_N$:

$$I_{tE}^{dq} = (Z_{ti}^{dq})^{-1}(u_E^{dq} - V_r^{dq}), \tag{89}$$

which gives (78e).

Substituting (84) and (88) into (80):

$$-i\omega_{0}V_{i,ref}^{dq} + \frac{1}{C_{ti}}(Z_{ti}^{dq})^{-1}(u_{Ei}^{dq} - V_{i,ref}^{dq}) - \frac{1}{C_{ti}}\bar{I}_{Li}^{dq} - \frac{1}{C_{ti}}\sum_{l \in \mathcal{E}_{i}}\mathcal{B}_{il}I_{El}^{dq} = 0.$$

$$(90)$$

Multiplying through by C_{ti} :

$$-i\omega_{0}C_{ti}V_{i,ref}^{dq} + (Z_{ti}^{dq})^{-1}(u_{Ei}^{dq} - V_{i,ref}^{dq}) - I_{Li}^{dq} - \sum_{l \in \mathcal{E}_{i}} \mathcal{B}_{il}I_{El}^{dq} = 0.$$
(91)

Rearranging:

$$(Z_{ti}^{dq})^{-1}(u_{Ei}^{dq} - V_{i,ref}^{dq}) = i\omega_0 C_{ti} V_{i,ref}^{dq} + I_{Li}^{dq} + \sum_{l \in \mathcal{E}_i} \mathcal{B}_{il} I_{El}^{dq}.$$
(92)

Multiplying both sides by Z_{ti}^{dq} :

$$u_{Ei}^{dq} - V_{i,ref}^{dq} = Z_{ti}^{dq} \left(i\omega_0 C_{ti} V_{i,ref}^{dq} + I_{Li}^{dq} + \sum_{l \in \mathcal{E}_i} \mathcal{B}_{il} I_{El}^{dq} \right). \tag{93}$$

Therefore.

$$u_{Ei}^{dq} = V_{i,ref}^{dq} + Z_{ti}^{dq} \left(i\omega_0 C_{ti} V_{i,ref}^{dq} + I_{Li}^{dq} + \sum_{l \in \mathcal{E}_i} \mathcal{B}_{il} I_{El}^{dq} \right). \tag{94}$$

Vectorizing (94) for all DGs $i \in \mathbb{N}_N$:

$$u_E^{dq} = V_r + Z_{ti}^{dq} \Big(\Omega_0 C_{ti} V_r + I_L + \mathcal{B}_D I_{El}^{dq} \Big),$$
 (95)

which gives (78f).

For each distribution line Σ_l^{line} , setting $\dot{\bar{x}}_l = 0$ in (17):

$$\left(\frac{R_l}{L_l} + i\omega_0\right)I_{El}^{dq} = \frac{1}{L_l} \sum_{k \in \mathcal{N}^P} \mathcal{B}_{kl} V_{Ek}^{dq},\tag{96}$$

where \mathcal{N}_l^P includes both DG and load nodes connected to line l. Multiplying both sides by L_l :

$$(R_l + i\omega_0 L_l)I_{El}^{dq} = \sum_{k \in \mathcal{N}_l^P} \mathcal{B}_{kl} V_{Ek}^{dq}.$$
 (97)

Using the complex impedance notation $Z_l^{dq} \triangleq R_l + i\omega_0 L_l$:

$$I_{El}^{dq} = (Z_l^{dq})^{-1} \sum_{k \in \mathcal{N}_l^P} \mathcal{B}_{kl} V_{Ek}^{dq}.$$
 (98)

Vectorizing for all lines $l \in \mathbb{N}_L$, we recognize that the summation over neighbor nodes $k \in \mathcal{N}_l^P$ corresponds to the incidence matrix operation. Since the incidence matrix \mathcal{B} has rows for both DGs (first N rows) and loads (next M rows), the full voltage vector includes both DG and load voltages:

$$I_{El}^{dq} = (Z_l^{dq})^{-1} \mathcal{B}^{\top} \begin{bmatrix} V_{dq}^{dq} \\ V_{mE}^{dq} \end{bmatrix}. \tag{99}$$

Using the partition $\mathcal{B} = \begin{bmatrix} \mathcal{B}_D^\top & \mathcal{B}_L^\top \end{bmatrix}^\top$:

$$I_{El}^{dq} = (Z_l^{dq})^{-1} \mathcal{B}_D^{\top} V_E^{dq} + (Z_l^{dq})^{-1} \mathcal{B}_L^{\top} V_{mE}^{dq}, \tag{100}$$

which gives (78c).

For each load subsystem Σ_m^{Load} , setting $\dot{V}_m^{dq}=0$ in (12):

$$-\mathrm{i}\omega_{0}V_{mE}^{dq} - \frac{1}{C_{tm}}(Y_{Lm}V_{mE}^{dq} + \bar{I}_{Lm}^{dq}) - \frac{1}{C_{tm}}\sum_{l \in \mathcal{E}_{m}}\mathcal{B}_{ml}I_{El}^{dq} = 0. \tag{101}$$

Multiplying through by C_{tm} :

$$-i\omega_0 C_{tm} V_{mE}^{dq} - Y_{Lm} V_{mE}^{dq} + \bar{I}_{Lm}^{dq} - \sum_{l \in \mathcal{E}_m} \mathcal{B}_{ml} I_{El}^{dq} = 0.$$
 (102)

Rearranging:

$$-(Y_{Lm} + i\omega_0 C_{tm})V_{mE}^{dq} = \bar{I}_{Lm}^{dq} + \sum_{l \in \mathcal{E}_m} \mathcal{B}_{ml}I_{El}^{dq}.$$
 (103)

Using the effective admittance notation $Y_{mE}^{dq} \triangleq Y_{Lm} + i\omega_0 C_{tm}$:

$$V_{mE}^{dq} = -(Y_m^{dq})^{-1} \left(\bar{I}_{Lm}^{dq} + \sum_{l \in \mathcal{E}_m} \mathcal{B}_{ml} I_{El}^{dq} \right). \tag{104}$$

Vectorizing for all loads $m \in \mathbb{N}_M$

$$V_{mE}^{dq} = -(Y_m^{dq})^{-1} \left(\bar{I}_{Lm}^{dq} + \mathcal{B}_L I_{El}^{dq} \right), \tag{105}$$

which gives (78d).

This completes the proof. The coupled (78a)-(78f) uniquely determines all equilibrium state variables.

Remark 4: The equilibrium analysis reveals the coupling between DG, line, and load dynamics through the complex impedance and admittance matrices $Z_l^{dq}, \ Z_{ti}^{dq}, \ \text{and} \ Y_m^{dq},$ which naturally incorporates the dq-frame cross-coupling through the $i\omega_0$ terms. The coupled equilibrium system has a unique solution since: (i) the complex impedance matrix $Z_l^{dq} = R_l + \mathrm{i}\omega_0 L_l$ is invertible for all physical line parameters with $R_l > 0$ and $L_l > 0$, as each diagonal block has a determinant $det(R_l + i\omega_0 L_l \mathbf{I}_2) = R_l^2 + \omega_0^2 L_l^2 > 0$; (ii) the effective admittance matrix $Y_m^{dq} = Y_{Lm} + \mathrm{i}\omega_0 C_{tm}$ is invertible for passive loads with $Y_{Lm}>0$ and $C_{tm}>0$; (iii) the filter impedance matrix $Z_{ti}^{dq}=R_{ti}+\mathrm{i}\omega_0L_{ti}$ is invertible with $\det(R_{ti}+\mathrm{i}\omega_0L_{ti}\mathbf{I}_2)=R_{ti}^2+\omega_0^2L_{ti}^2>0$; and (iv) the interconnection structure through the incidence matrix \mathcal{B} is determined by the connected AC MG topology. Therefore, the equilibrium state $(V_E^{dq}, I_{tE}^{dq}, I_{El}^{dq}, V_{mE}^{dq}, \tilde{\omega}_E)$ exists and is unique for any given reference voltage V_r , constant current loads \bar{I}_L and \bar{I}_m , and system parameters. The control input u_E^{dq} is then uniquely determined by (78f).

Remark 5: At equilibrium, to achieve proportional active and reactive power sharing among DG units, we require:

$$\frac{P_{Ei}}{P_i^{\max}} = P_{n,Ei} = P_{n,Ej} = \frac{P_{Ej}}{P_j^{\max}}, \quad \forall i, j \in \mathbb{N}_N,$$

$$\frac{Q_{Ei}}{Q_i^{\max}} = Q_{n,Ei} = Q_{n,Ej} = \frac{Q_{Ej}}{Q_j^{\max}}, \quad \forall i, j \in \mathbb{N}_N,$$
(106)

where P_i^{\max} and Q_i^{\max} are the power ratings of Σ_i^{DG} . This relationship ensures that the steady-state distributed control input is:

$$u_{EiG}^{dq} = \begin{bmatrix} u_{Ei}^P \\ u_{Ei}^Q \end{bmatrix} = \begin{bmatrix} K_{ij}^P \sum_{j \in \mathcal{N}_i^C} (P_{n,Ei} - P_{n,Ej}) \\ K_{ij}^Q \sum_{j \in \mathcal{N}_i^C} (Q_{n,Ei} - Q_{n,Ej}) \end{bmatrix} = \mathbf{0}.$$
(107)

VI. DISSIPATIVITY-BASED CONTROL AND TOPOLOGY Co-DESIGN

This section analyzes the dissipativity properties of the AC MG error subsystems and formulates the global control and topology co-design problem. We establish necessary conditions for subsystem passivity indices and synthesize local controllers to ensure global feasibility.

Consider the DG error subsystem $\tilde{\Sigma}_i^{DG}, i \in \mathbb{N}_N$ from (57)

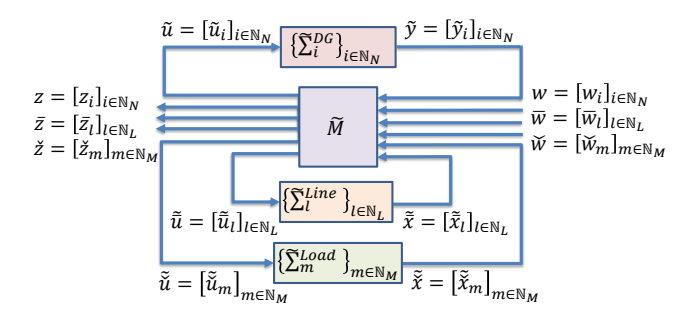


Fig. 6. Error networked system configuration showing interconnections between DGs, lines, and loads error dynamics in AC MG.

as an X_i -EID with

$$X_{i} = \begin{bmatrix} X_{i}^{11} & X_{i}^{12} \\ X_{i}^{21} & X_{i}^{22} \end{bmatrix} \triangleq \begin{bmatrix} -\nu_{i} \mathbf{I} & \frac{1}{2} \mathbf{I} \\ \frac{1}{2} \mathbf{I} & -\rho_{i} \mathbf{I} \end{bmatrix},$$
(108)

where ρ_i and ν_i are the passivity indices of $\tilde{\Sigma}_i^{DG}$, i.e., $\tilde{\Sigma}_i^{DG}, i \in \mathbb{N}_N$ is IF-OFP (ν_i, ρ_i) .

Similarly, the line subsystem $\tilde{\Sigma}_l^{Line}$, $l \in \mathbb{N}_L$ from (64), is assumed to be \bar{X}_l -EID with

$$\bar{X}_{l} = \begin{bmatrix} \bar{X}_{l}^{11} & \bar{X}_{l}^{12} \\ \bar{X}_{l}^{21} & \bar{X}_{l}^{22} \end{bmatrix} \triangleq \begin{bmatrix} -\bar{\nu}_{l} \mathbf{I} & \frac{1}{2} \mathbf{I} \\ \frac{1}{2} \mathbf{I} & -\bar{\rho}_{l} \mathbf{I} \end{bmatrix}, \tag{109}$$

where $\bar{\rho}_l$ and $\bar{\nu}_l$ are the line passivity indices

Additionally, the load error subsystem $\tilde{\Sigma}_m^{Load}, m \in \mathbb{N}_M$ from (66), is assumed to be X_m -EID with

$$\check{X}_{m} = \begin{bmatrix}
\check{X}_{m}^{11} & \check{X}_{m}^{12} \\
\check{X}_{m}^{21} & \check{X}_{m}^{22}
\end{bmatrix} \triangleq \begin{bmatrix}
-\check{\nu}_{m}\mathbf{I} & \frac{1}{2}\mathbf{I} \\
\frac{1}{2}\mathbf{I} & -\check{\rho}_{m}\mathbf{I}
\end{bmatrix},$$
(110)

where $\check{\rho}_m$ and $\check{\nu}_m$ are the load passivity indices.

Lemma 2: For $\tilde{\Sigma}_{l}^{Line}$, $l \in \mathbb{N}_{L}$ (64), the passivity indices $\bar{\nu}_l$, and $\bar{\rho}_l$ satisfy the LMI:

Find: \bar{P}_l , $\bar{\nu}_l$, and $\bar{\rho}_l$

$$\text{s.t.: } \bar{P}_l > 0, \ \begin{bmatrix} \frac{2\bar{P}_lR_l}{L_l} - \bar{\rho}_l\mathbf{I}_2 & -\frac{\bar{P}_l}{L_l} + \frac{1}{2}\mathbf{I}_2 \\ \star & -\bar{\nu}_l\mathbf{I}_2 \end{bmatrix} \geq 0,$$
 with maximum feasible values $\bar{\nu}_l^{\max} = 0$ and $\bar{\rho}_l^{\max} = R_l\mathbf{I}_2$

when $\bar{P}_l = \frac{L_l}{2} \mathbf{I}_2$.

Proof: For $\tilde{\Sigma}_{l}^{Line}$, $l \in \mathbb{N}_{L}$ described by (64), we need to ensure it is \bar{X}_l -dissipative with the passivity indices defined in (109). Applying Prop. 1 with the system matrices from (19) and the dissipativity supply rate form in (109) yields the LMI condition (111).

Using the Schur complement, this is positive semidefinite if and only if:

1)
$$\bar{\nu}_l < 0$$
.

2)
$$2\bar{P}_{l}\frac{R_{l}}{L_{l}} - \bar{\rho}_{l}\mathbf{I}_{2} - \frac{(-\bar{P}_{l}\frac{1}{L_{l}} + \frac{1}{2}\mathbf{I}_{2})^{2}}{-\bar{\nu}_{l}} \ge 0.$$
 (112)

To maximize the passivity indices, we set $\bar{\nu}_l = 0$, which gives:

1)
$$2\bar{P}_{l}\frac{R_{l}}{L_{l}} - \bar{\rho}_{l}\mathbf{I}_{2} \ge 0,$$

2) $-\bar{P}_{l}\frac{1}{L_{l}} + \frac{1}{2}\mathbf{I}_{2} = 0,$ (113)

Substituting this into condition 1 gives $R_l \mathbf{I}_2 - \bar{\rho}_l \mathbf{I}_2 \geq 0$, implying $\bar{\rho}_l \leq R_l \mathbf{I}_2$. Therefore, the maximum feasible values are $\bar{\nu}_l^{\max} = 0$ and $\bar{\rho}_l^{\max} = R_l \mathbf{I}_2$ when $\bar{P}_l = \frac{L_l}{2} \mathbf{I}_2$.

Lemma 3: For $\tilde{\Sigma}_{m}^{Load}$, $m \in \mathbb{N}_{M}$ (66), the passivity indices

 $\check{\nu}_m$ and $\check{\rho}_m$ satisfy the LMI:

Find: \check{P}_m , $\check{\nu}_m$, and $\check{\rho}_m$

s.t.:
$$\check{P}_m > 0$$
, $\begin{bmatrix} \frac{2\check{P}_m Y_{Lm}}{C_{tm}} - \check{\rho}_m \mathbf{I}_2 & -\frac{\check{P}_m}{C_{tm}} + \frac{1}{2} \mathbf{I}_2 \\ \star & -\check{\nu}_m \mathbf{I}_2 \end{bmatrix} \ge 0$, (114)

with maximum feasible values $\check{
u}_m^{\max} = 0$ and $\check{
ho}_l^{\max} = Y_{Lm} \mathbf{I}_2$ when $\check{P}_m = \frac{C_{tm}}{2} \mathbf{I}_2$.

Proof: For $\tilde{\Sigma}_m^{Load}$, $m \in \mathbb{N}_M$ described by (66), we need to ensure it is \check{X}_m -dissipative with the passivity indices defined in (110). Applying Prop. 1 with the system matrices from (15) and the dissipativity supply rate form in (110) vields the LMI condition (114).

Using the Schur complement, this is positive semidefinite if and only if:

1)
$$\check{\nu}_m \leq 0$$
,

2)
$$2\check{P}_m \frac{Y_{Lm}}{C_{tm}} - \check{\rho}_m \mathbf{I}_2 - \frac{(-\frac{\check{P}_m}{C_{tm}} + \frac{1}{2}\mathbf{I}_2)^2}{-\check{\nu}_m} \ge 0.$$
 (115)

To maximize the passivity indices, we set $\check{\nu}_m = 0$, which

1)
$$2\check{P}_{m}\frac{Y_{Lm}}{C_{tm}} - \check{\rho}_{m}\mathbf{I}_{2} \ge 0,$$

2) $-\frac{\check{P}_{m}}{C_{tm}} + \frac{1}{2}\mathbf{I}_{2} = 0.$ (116)

Substituting this into condition 1 gives $Y_{Lm}\mathbf{I}_2 - \check{\rho}_m\mathbf{I}_2 \ge 0$, implying $\check{\rho}_m \leq Y_{Lm}\mathbf{I}_2$. Therefore, the maximum feasible values are $\check{\nu}_m^{\max} = 0$ and $\check{\rho}_m^{\max} = Y_{Lm}\mathbf{I}_2$ when $\check{P}_m = \frac{C_{tm}}{2}\mathbf{I}_2$.

A. Frequency Coupling Nonlinearity

The frequency coupling nonlinearity in the DG error dynamics (57) arises from the cross-coupling between dand q axes in the synchronously rotating reference frame. This nonlinearity must be rigorously characterized to enable systematic controller synthesis within the LMI framework.

The following lemmas establish a quadratic constraint to capture the nonlinearity, convert it to a suitable quadratic form, and incorporate it into the dissipativity-based controller design through the S-procedure.

Lemma 4: For the frequency coupling nonlinearity $q_i(\tilde{x}_i)$ defined in (60), there exists a scalar $\gamma_i \triangleq \sqrt{C_{ti}^2 \bar{V}_{tot}^2 + \bar{L}_{ti}^2 \bar{I}_{tot}^2}$ (where $\bar{V}_{tot} = \bar{V} + \|V_{iE}^{dq}\|$ and $\bar{I}_{tot} = \bar{I} + \|I_{tiE}^{dq}\|$) such that for all \tilde{x}_i in the operating region, the norm bound

$$||g_i(\tilde{x}_i)||^2 \le \tilde{\omega}_i^2 \cdot \tilde{\gamma}^2, \tag{117}$$

holds, which is equivalent to the quadratic constraint

$$\begin{bmatrix} \tilde{x}_i \\ g_i(\tilde{x}_i) \end{bmatrix}^\top \Psi_i \begin{bmatrix} \tilde{x}_i \\ g_i(\tilde{x}_i) \end{bmatrix} \ge 0, \tag{118}$$

where:

$$\Psi_i = \begin{bmatrix} \gamma_i^2 e_7 e_7^\top & \mathbf{0}_{7\times7} \\ \mathbf{0}_{7\times7} & -\mathbf{I}_7 \end{bmatrix} \in \mathbb{R}^{14\times14}, \tag{119}$$

and $e_7 = \begin{bmatrix} 0 & 0 & 0 & 0 & 0 & 1 \end{bmatrix}^{\top} \in \mathbb{R}^7$ extracts the frequency error component $\tilde{\omega}_i$ from \tilde{x}_i .

Proof: The frequency coupling nonlinearity has the structure in (60), which yields the following:

$$||g_i(\tilde{x}_i)||^2 = \tilde{\omega}_i^2 \left[||V_i^{dq}||^2 + ||I_{t_i}^{dq}||^2 \right].$$
 (120)

Using the error variable definitions (55a)-(55b) and traingle inequality in the operating region where $\|\tilde{V}_i^{dq}\| \leq \bar{V}$ and $\|\tilde{I}_{ti}^{dq}\| \leq \bar{I}$, we obtain $\|V_i^{dq}\| \leq \bar{V}_{tot}$ and $\|I_{ti}^{dq}\| \leq \bar{I}_{tot}$. With the physical system parameters C_{ti} and L_{ti} to weight the voltage and current contributions, this establishes:

 $||g_i(\tilde{x}_i)||^2 \le \tilde{\omega}_i^2 \left[C_{ti}^2 \bar{V}_{tot}^2 + L_{ti}^2 \bar{I}_{tot}^2 \right] = \tilde{\omega}_i^2 \cdot \gamma_i^2,$ which is equation (117). Rearranging (117) gives $\gamma_i^2 \tilde{\omega}_i^2$ – $||g_i(\tilde{x}_i)||^2 \geq 0$, and since $\tilde{\omega}_i = e_7^{\top} \tilde{x}_i$, expanding the quadratic form yields

$$\begin{bmatrix} \tilde{x}_i \\ g_i(\tilde{x}_i) \end{bmatrix}^{\top} \Psi_i \begin{bmatrix} \tilde{x}_i \\ g_i(\tilde{x}_i) \end{bmatrix} = \tilde{x}_i^{\top} (\gamma_i^2 e_7 e_7^{\top}) \tilde{x}_i + g_i(\tilde{x}_i)^{\top} (-\mathbf{I}_7) g_i(\tilde{x}_i)$$
$$= \gamma_i^2 (e_7^{\top} \tilde{x}_i)^2 - \|g_i(\tilde{x}_i)\|^2 = \gamma_i^2 \tilde{\omega}_i^2 - \|g_i(\tilde{x}_i)\|^2,$$

establishing the equivalence between (117) and (118) and completing the proof.

Lemma 5: Consider a quadratic storage $V_i(\tilde{x}_i) = \tilde{x}_i^{\top} P_i \tilde{x}_i$ with $P_i > 0$. If there exist $\lambda_i > 0$ and $R_i = R_i^{\top}$ such that,

$$\begin{bmatrix} R_i & -P_i \\ -P_i & \mathbf{0}_{7\times7} \end{bmatrix} - \lambda_i \Psi_i \ge 0, \tag{122}$$

where Ψ_i is defined in (119), then the nonlinearity term in the storage function derivative satisfies:

$$2\tilde{x}_i^{\top} P_i g_i(\tilde{x}_i) \le \tilde{x}_i^{\top} R_i \tilde{x}_i. \tag{123}$$

Proof: From Lm. 4, we know that for all \tilde{x}_i in the operating region:

$$\begin{bmatrix} \tilde{x}_i \\ g_i(\tilde{x}_i) \end{bmatrix}^{\top} \Psi_i \begin{bmatrix} \tilde{x}_i \\ g_i(\tilde{x}_i) \end{bmatrix} \ge 0. \tag{124}$$

By the S-procedure (S-lemma), if there exists $\lambda_i > 0$ such that condition (122) holds, then for all \tilde{x}_i , $g_i(\tilde{x}_i)$ satisfies the constraint in Lemma 4:

$$\begin{bmatrix} \tilde{x}_i \\ g_i(\tilde{x}_i) \end{bmatrix}^{\top} \begin{bmatrix} R_i & -P_i \\ -P_i & \mathbf{0}_{7\times7} \end{bmatrix} \begin{bmatrix} \tilde{x}_i \\ g_i(\tilde{x}_i) \end{bmatrix} \ge 0. \tag{125}$$

$$\tilde{x}_i^\top R_i \tilde{x}_i + \tilde{x}_i^\top (-P_i) g_i(\tilde{x}_i) + g_i(\tilde{x}_i)^\top (-P_i) \tilde{x}_i + g_i(\tilde{x}_i)^\top \mathbf{0} \cdot g_i(\tilde{x}_i)$$

Simplifying (using $\tilde{x}_i^{\top} P_i g_i = g_i^{\top} P_i \tilde{x}_i$ since P_i is symmetric):

$$\tilde{x}_i^{\top} R_i \tilde{x}_i - 2 \tilde{x}_i^{\top} P_i g_i(\tilde{x}_i) \ge 0.$$

Rearranging:

$$2\tilde{x}_i^{\top} P_i g_i(\tilde{x}_i) \leq \tilde{x}_i^{\top} R_i \tilde{x}_i.$$

This completed the proof.

Lemma 6: If there exist $\tilde{\lambda}_i > 1$ and $\tilde{R}_i = \tilde{R}_i^{\top} > 0$ such

$$\Phi_{i} \triangleq \begin{bmatrix} \mathbf{I} & \mathbf{0} & \mathbf{0} \\ \mathbf{0} & \tilde{P}_{i}e_{7} & \mathbf{0} \end{bmatrix} + \begin{bmatrix} \mathbf{I} & \mathbf{0} \\ \mathbf{0} & e_{7}^{\top}\tilde{P}_{i} \\ \mathbf{0} & \mathbf{0} \end{bmatrix} - \begin{bmatrix} \tilde{R}_{i} & \mathbf{0} \\ \mathbf{0} & \mathbf{I} \end{bmatrix} - \begin{bmatrix} \tilde{R}_{i} & \mathbf{0} \\ \mathbf{0} & \mathbf{I} \end{bmatrix} - \begin{bmatrix} \tilde{R}_{i} & \mathbf{0} \\ \mathbf{0} & \mathbf{I} \end{bmatrix} - \begin{bmatrix} \tilde{R}_{i} & \mathbf{0} \\ \mathbf{0} & \mathbf{I} \end{bmatrix} - \begin{bmatrix} \tilde{R}_{i} & \mathbf{0} \\ \mathbf{0} & \mathbf{I} \end{bmatrix} - \begin{bmatrix} \tilde{R}_{i} & \mathbf{0} \\ \mathbf{0} & \mathbf{I} \end{bmatrix} \geq \mathbf{0},$$

then the quadratic bound (122) from Lemma 5 holds, where $P_i = \tilde{P}_i^{-1}$, $R_i = \tilde{R}_i^{-1}$, $\lambda_i = \tilde{\lambda}_i^{-1}$, e_7 , and Ψ_i are defined in Lemma 4.

Proof: From Lemma 5, expanding (122) using the

structure of Ψ_i defined in (119):

$$\begin{bmatrix} R_i - \lambda_i \gamma_i^2 e_7 e_7^\top & -P_i \\ -P_i & \lambda_i \mathbf{I}_7 \end{bmatrix} \ge 0.$$

To obtain an LMI in design variables compatible with controller synthesis, we apply the change of variables:

$$P_i = \tilde{P}_i^{-1}, \ R_i = \tilde{R}_i^{-1}, \ \lambda_i = \tilde{\lambda}_i^{-1}.$$
 (127)

Using Corollary 1, the first three terms in Φ_i satisfy:

quadratic form yields
$$\begin{bmatrix} \tilde{x}_i \\ g_i(\tilde{x}_i) \end{bmatrix}^\top \Psi_i \begin{bmatrix} \tilde{x}_i \\ g_i(\tilde{x}_i) \end{bmatrix} = \tilde{x}_i^\top (\gamma_i^2 e_7 e_7^\top) \tilde{x}_i + g_i(\tilde{x}_i)^\top (-\mathbf{I}_7) g_i(\tilde{x}_i), \begin{bmatrix} \mathbf{I} & \mathbf{0} & \mathbf{0} \\ \mathbf{0} & \tilde{P}_i e_7 & \mathbf{0} \end{bmatrix} + \begin{bmatrix} \mathbf{I} & \mathbf{0} \\ \mathbf{0} & e_7^\top \tilde{P}_i \\ \mathbf{0} & \mathbf{0} \end{bmatrix} - \begin{bmatrix} \tilde{R}_i & \mathbf{0} \\ \mathbf{0} & \mathbf{I} \end{bmatrix} \leq \begin{bmatrix} R_i & \mathbf{0} \\ \mathbf{0} & \tilde{P}_i e_7 e_7^\top \tilde{P}_i \end{bmatrix}.$$

Therefore, Ψ_i is upper bounded as:

$$\Phi_i \leq \begin{bmatrix} R_i - \gamma_i^2 \tilde{P}_i e_7 e_7^\top \tilde{P}_i & -\tilde{\lambda}_i \mathbf{I} \\ -\tilde{\lambda}_i \mathbf{I} & \tilde{P}_i e_7 e_7^\top \tilde{P}_i \end{bmatrix}.$$

Since $\tilde{\lambda}_i > 1$ implies $\lambda_i < 1$, we have:

$$\frac{1}{\tilde{\lambda}_i}\Phi_i \leq \frac{1}{\tilde{\lambda}_i} \begin{bmatrix} \mathbf{I} & \mathbf{0} \\ \mathbf{0} & \tilde{P}_i \end{bmatrix} \left(\begin{bmatrix} R_i & -P_i \\ -P_i & \mathbf{0} \end{bmatrix} - \lambda_i \Psi_i \right) \begin{bmatrix} \mathbf{I} & \mathbf{0} \\ \mathbf{0} & \tilde{P}_i \end{bmatrix} \triangleq \bar{\Phi}_i.$$

Combining (126), $\bar{\Phi}_i \geq \Phi_i$, $\tilde{P}_i > 0$, $\tilde{\lambda}_i > 0$, and the implication from Lemma 5:

$$(126) \iff \Phi_i \ge \mathbf{0} \implies \bar{\Phi}_i \ge 0 \iff (122) \implies (122).$$

Theorem 1: Under the quadratic constraint on the frequency coupling nonlinearity established in Lemma 4 and the tractable LMI form established in Lemma 6, the DG error subsystem $\tilde{\Sigma}_i^{DG}: \tilde{u}_i \to \tilde{x}_i, i \in \mathbb{N}_N$ (57) can be made IF-OFP(ν_i, ρ_i) (as assumed in (108)) by designing the local controller gain matrix K_{i0} (21) via solving the LMI problem:

Find: \tilde{K}_{i0} , \tilde{P}_i , \tilde{R}_i , $\tilde{\lambda}_i$, ν_i , and $\tilde{\rho}_i$,

s.t.:
$$\tilde{P}_i > 0, \ \tilde{R}_i > 0, \ \tilde{\lambda}_i > 1,$$

$$\begin{bmatrix} g_i(\tilde{x}_i) \end{bmatrix} \quad \begin{bmatrix} -P_i & \mathbf{0}_{7 \times 7} \end{bmatrix} \quad \begin{bmatrix} g_i(\tilde{x}_i) \end{bmatrix} \geq 0.$$
 (123) Similarly 50, Te_i > 0, Te_i > 0

where $K_{i0} \triangleq \tilde{K}_{i0}\tilde{P}_i^{-1}$, $\rho_i \triangleq \frac{1}{\tilde{\rho}_i}$, e_7 , and γ_i are defined in Lemma 4.

Proof: The second LMI constraint in Theorem 1 directly follows from Lemma 6, which ensures that the quadratic bound (122) from Lemma 5 holds. Therefore, we focus on establishing the first LMI constraint in Theorem 1.

Consider a quadratic storage function $V_i(\tilde{x}_i) = \tilde{x}_i^{\top} P_i \tilde{x}_i$, where $P_i > 0$. The derivative of the storage function along the system trajectory (57) is:

$$\dot{\mathbf{V}}_i(\tilde{x}_i) = 2\tilde{x}_i^{\top} P_i(\hat{A}_i \tilde{x}_i + g_i(\tilde{x}_i) + \tilde{u}_i), \qquad (129)$$
 where $\hat{A}_i \triangleq A_i + B_i K_{i0}$.

Applying the bound (122) from Lemma 5:

$$\dot{\mathbf{V}}_{i}(\tilde{x}_{i}) \leq 2\tilde{x}_{i}^{\top} P_{i} \hat{A}_{i} \tilde{x}_{i} + \tilde{x}_{i}^{\top} R_{i} \tilde{x}_{i} + 2\tilde{x}_{i}^{\top} P_{i} \tilde{u}_{i},
= \tilde{x}_{i}^{\top} (\mathcal{H}(P_{i} A_{i} + P_{i} B_{i} K_{i0}) + R_{i}) \tilde{x}_{i} + 2\tilde{x}_{i}^{\top} P_{i} \tilde{u}_{i}. \tag{130}$$

For the IF-OFP (ν_i, ρ_i) property (108), we require:

$$\dot{\mathbf{V}}_{i}(\tilde{x}_{i}) \leq \begin{bmatrix} \tilde{u}_{i} \\ \tilde{x}_{i} \end{bmatrix}^{\top} \begin{bmatrix} -\nu_{i} \mathbf{I} & \frac{1}{2} \mathbf{I} \\ \frac{1}{2} \mathbf{I} & -\rho_{i} \mathbf{I} \end{bmatrix} \begin{bmatrix} \tilde{u}_{i} \\ \tilde{x}_{i} \end{bmatrix}. \tag{131}$$

Combining (130) and (131), we obtain:

$$\begin{bmatrix} \tilde{x}_i \\ \tilde{u}_i \end{bmatrix}^\top \Omega_i \begin{bmatrix} \tilde{x}_i \\ \tilde{u}_i \end{bmatrix} \ge 0, \tag{132}$$

where:

$$\Omega_{i} \triangleq \begin{bmatrix} -\mathcal{H}(P_{i}A_{i} + P_{i}B_{i}K_{i0}) - (R_{i} + \rho_{i}\mathbf{I}) & \frac{1}{2}\mathbf{I} - P_{i} \\ \frac{1}{2}\mathbf{I} - P_{i} & -\nu_{i}\mathbf{I} \end{bmatrix} \geq 0.$$
(133)

Since P_i and K_{i0} form a bilinear term in (133), we preand post-multiply Ω_i by $\operatorname{diag}([P_i^{-1},\mathbf{I}])$ where $\tilde{P}_i=P_i^{-1}$, and apply the change of variables $\tilde{K}_{i0}=K_{i0}\tilde{P}_i$ to obtain:

$$\begin{bmatrix} -\mathcal{H}(A_i\tilde{P}_i + B_i\tilde{K}_{i0}) - \tilde{P}_i(R_i + \rho_i\mathbf{I})\tilde{P}_i & \frac{1}{2}\tilde{P}_i - \mathbf{I} \\ \frac{1}{2}\tilde{P}_i - \mathbf{I} & -\nu_i\mathbf{I} \end{bmatrix} \ge 0.$$
(134)

Assuming $R_i + \rho_i \mathbf{I} > 0$ (which is justified in Assumption 1 and Lemma 6 and applying matrix inversion, we have:

$$(R_i + \rho_i I)^{-1} = R_i^{-1} - R_i^{-1} (\rho_i^{-1} \mathbf{I} + R_i^{-1})^{-1} R_i^{-1}.$$

Using the change of variables $\tilde{R}_i = R_i^{-1}$ and $\tilde{\rho}_i = \rho_i^{-1}$, and applying Schur complement, condition (134) is equivalent to:

$$\begin{bmatrix} (R_i + \rho_i \mathbf{I})^{-1} & \tilde{P}_i & \mathbf{0} \\ \tilde{P}_i & -H(A_i \tilde{P}_i + B_i \tilde{K}_{i0}) & \frac{1}{2} \tilde{P}_i - \mathbf{I} \\ \mathbf{0} & \frac{1}{2} \tilde{P}_i - \mathbf{I} & -\nu_i \mathbf{I} \end{bmatrix} \ge 0.$$

Applying Schur complement to expand $(R_i + \rho_i \mathbf{I})^{-1}$ in the above equation, and leveraging the fact that $\tilde{R}_i = R_i^{-1}$ and $\tilde{\rho}_i = \rho_i^{-1}$, we obtain through algebraic manipulation:

$$egin{bmatrix} ilde{
ho}_i\mathbf{I}+ ilde{R}_i & ilde{R}_i & \mathbf{0} & \mathbf{0} \ ilde{R}_i & ilde{R}_i & ilde{P}_i & \mathbf{0} \ \mathbf{0} & ilde{P}_i & -H(A_i ilde{P}_i+B_i ilde{K}_{i0}) & -\mathbf{I}+rac{1}{2} ilde{P}_i \ \mathbf{0} & \mathbf{0} & -\mathbf{I}+rac{1}{2} ilde{P}_i & -
u_i\mathbf{I} \ \end{bmatrix} \geq \mathbf{0},$$

This completes the proof.

B. Global Control and Topology Co-design

The local controllers (21) regulate voltages of individual DGs while ensuring that closed-loop DG dynamics satisfy the required dissipativity properties. Given these subsystem properties, we now synthesize the interconnection matrix \tilde{M} (21) (see Fig. 6), particularly its block \tilde{K} , using Proposition 2. Note that, by synthesizing $K = [K_{ij}]_{i,j \in \mathbb{N}_N}$, we can uniquely determine the consensus-based distributed global controller $\{K_{ij}^P, K_{ij}^Q: i, j \in \mathbb{N}_N\}$ (28), along with the required communication topology \mathcal{G}^c . Note also that, when designing \tilde{K} , we particularly enforce the closed-loop AC MG error dynamics to be **Y**-dissipative with $\mathbf{Y} \triangleq \begin{bmatrix} \gamma^2 \mathbf{I} & \mathbf{0} \\ \mathbf{0} & -\mathbf{I} \end{bmatrix}$ (see Remark 1) to prevent/bound the amplification of disturbances affecting the performance. The following theorem formulates this distributed global controller and communication topology co-design problem.

Theorem 2: The closed-loop networked error dynamics of the AC MG (see Fig. 6) can be made finite-gain L_2 -stable with an L_2 gain γ from disturbance $w_c(t)$ to performance output $z_c(t)$ (where $\tilde{\gamma} \triangleq \gamma^2 < \bar{\gamma}$ is prespecified), by synthesizing the interconnection matrix block $\tilde{M}_{\tilde{u}x} = K$ (77) via solving the LMI problem:

$$\min_{\substack{Q,\{p_i: i \in \mathbb{N}_N\}, \\ \{\bar{p}_i: l \in \mathbb{N}_L\}, \tilde{\gamma}}} \sum_{i,j \in \mathbb{N}_N} c_{ij} \|Q_{ij}\|_1 + c_0 \tilde{\gamma},$$
Sub. to:
$$p_i > 0, \ \bar{p}_l > 0, \ \check{p}_m > 0,$$

$$0 < \tilde{\gamma} < \bar{\gamma}, \text{ and the LMI (136)},$$

$$(135)$$

Here $K = (\mathbf{X}_p^{11})^{-1}Q$, $\mathbf{X}^{12} \triangleq \operatorname{diag}([-\frac{1}{2\nu_i}\mathbf{I}]_{i\in\mathbb{N}_N})$, $\mathbf{X}^{21} \triangleq (\mathbf{X}^{12})^{\top}$, $\bar{\mathbf{X}}^{12} \triangleq \operatorname{diag}([-\frac{1}{2\bar{\nu}_l}\mathbf{I}]_{l\in\mathbb{N}_L})$, $\bar{\mathbf{X}}^{21} \triangleq (\bar{\mathbf{X}}^{12})^{\top}$, $\bar{\mathbf{X}}^{12} \triangleq \operatorname{diag}([-\frac{1}{2\bar{\nu}_m}\mathbf{I}]_{m\in\mathbb{N}_M})$, $\bar{\mathbf{X}}^{21} \triangleq (\bar{\mathbf{X}}^{12})^{\top}$, $\mathbf{X}_p^{11} \triangleq \operatorname{diag}([-p_i\nu_i\mathbf{I}]_{i\in\mathbb{N}_N})$, $\mathbf{X}_p^{22} \triangleq \operatorname{diag}([-p_i\rho_i\mathbf{I}]_{i\in\mathbb{N}_N})$, $\bar{\mathbf{X}}_{\bar{p}}^{11} \triangleq \operatorname{diag}([-\bar{p}_l\bar{\nu}_l\mathbf{I}]_{l\in\mathbb{N}_L})$, $\bar{\mathbf{X}}_{\bar{p}}^{22} \triangleq \operatorname{diag}([-\bar{p}_l\bar{\rho}_l\mathbf{I}]_{l\in\mathbb{N}_L})$, $\bar{\mathbf{X}}_{\bar{p}}^{11} \triangleq \operatorname{diag}([-\check{p}_m\check{\nu}_m\mathbf{I}]_{m\in\mathbb{N}_M})$, $\bar{\mathbf{X}}_{\bar{p}}^{12} \triangleq \operatorname{diag}([-\check{p}_m\check{\rho}_m\mathbf{I}]_{m\in\mathbb{N}_M})$, and $\tilde{\Gamma} \triangleq \tilde{\gamma}\mathbf{I}$. The structure of $Q \triangleq [Q_{ij}]_{i,j\in\mathbb{N}_N}$ mirrors $K \triangleq [K_{ij}]_{i,j\in\mathbb{N}_N}$ (with zeros in appropriate blocks). The coefficients $c_0 > 0$ and $c_{ij} > 0$, $\forall i,j\in\mathbb{N}_N$ weight disturbance attenuation and communication costs.

C. Local Controller Synthesis

To enforce the necessary LMI conditions from Lemma ?? (??) on DG and line passivity indices and ensure numerical feasibility, we formalize the local controller synthesis problem as follows.

Theorem 3: Under the predefined DG parameters (35) and line parameters (19) with design parameters $\{p_i: i \in \mathbb{N}_N\}$ and $\{\bar{p}_l: l \in \mathbb{N}_L\}$, the necessary conditions for global co-design (135) hold if local controller gains $\{K_{i0}, i \in \mathbb{N}_N\}$ (21) and DG and line passivity indices $\{\nu_i, \rho_i: i \in \mathbb{N}_N\}$ (108) and $\{\bar{\nu}_l, \bar{\rho}_l: l \in \mathbb{N}_L\}$ (109) are determined:

$$\begin{split} & \text{Find: } \left\{ (\tilde{K}_{i0}, P_i, \nu_i, \tilde{\rho}_i, \tilde{\gamma}_i) : i \in \mathbb{N}_N \right\} \text{ and } \left\{ (\bar{P}_l, \bar{\nu}_l, \bar{\rho}_l) : l \in \mathbb{N}_L \right\} \\ & \text{s.t.: } -\frac{\tilde{\gamma}_i}{p_i} < \nu_i < 0, \ 0 < \tilde{\rho}_i < \min \left\{ p_i, \frac{4\tilde{\gamma}_i}{p_i} \right\}, \\ & P_i > 0, \begin{bmatrix} \bar{\rho}_i \mathbf{I} & P_i & \mathbf{0} \\ P_i & -\mathcal{H}(A_i P_i + B_i \tilde{K}_{i0}) & -\mathbf{I} + \frac{1}{2} P_i \\ \mathbf{0} & -\mathbf{I} + \frac{1}{2} P_i & -\nu_i \mathbf{I} \end{bmatrix} > 0, \ \forall i \in \mathbb{N}_N, \\ & \bar{P}_l > 0, \begin{bmatrix} \frac{2\bar{P}_l R_l}{L_l} - \bar{\rho}_l & -\frac{\bar{P}_l}{L_l} + \frac{1}{2} \\ & \star & -\bar{\nu}_l \end{bmatrix} \end{split}$$

and additional necessary conditions (??), where $K_{i0} \triangleq \tilde{K}_{i0}P_i^{-1}$ and $\rho_i \triangleq \frac{1}{\tilde{\rho}_i}$.

This unified LMI framework ensures local stability while guaranteeing feasibility of the global co-design, enabling systematic synthesis of the local controllers and the distributed communication topology.

VII. CONCLUSION

This paper proposes a dissipativity-based distributed control and communication topology co-design approach for AC MGs. By leveraging dissipativity theory, we develop a unified framework that simultaneously addresses distributed controller design and communication topology design problems using specifically designed local controllers and distributed

frequency synchronization through normalized power consensus. We formulate all design problems as LMI-based convex optimization problems to enable efficient solutions. The proposed approach ensures robust voltage regulation, frequency synchronization, and proportional power sharing while maintaining system stability through rigorous dissipativity analysis.

REFERENCES

- [1] Y. Han, H. Li, P. Shen, E. A. A. Coelho, and J. M. Guerrero, "Review of active and reactive power sharing strategies in hierarchical controlled microgrids," *IEEE Transactions on Power Electronics*, vol. 32, no. 3, pp. 2427–2451, 2016.
- [2] D. E. Olivares, A. Mehrizi-Sani, A. H. Etemadi, C. A. Cañizares, R. Iravani, M. Kazerani, A. H. Hajimiragha, O. Gomis-Bellmunt, M. Saeedifard, R. Palma-Behnke et al., "Trends in microgrid control," *IEEE Transactions on smart grid*, vol. 5, no. 4, pp. 1905–1919, 2014.
- [3] J. Rocabert, A. Luna, F. Blaabjerg, and P. Rodriguez, "Control of power converters in ac microgrids," *IEEE transactions on power* electronics, vol. 27, no. 11, pp. 4734–4749, 2012.
- [4] S. Sahoo, T. Dragičević, and F. Blaabjerg, "Cyber security in control of grid-tied power electronic converters—challenges and vulnerabilities," *IEEE Journal of Emerging and Selected Topics in Power Electronics*, vol. 9, no. 5, pp. 5326–5340, 2019.
- [5] A. Bidram and A. Davoudi, "Hierarchical structure of microgrids control system," *IEEE Transactions on Smart Grid*, vol. 3, no. 4, pp. 1963–1976, 2012.
- [6] Q. Shafiee, J. M. Guerrero, and J. C. Vasquez, "Distributed secondary control for islanded microgrids—a novel approach," *IEEE Transac*tions on power electronics, vol. 29, no. 2, pp. 1018–1031, 2013.
- [7] F. Guo, C. Wen, J. Mao, and Y.-D. Song, "Distributed secondary voltage and frequency restoration control of droop-controlled inverterbased microgrids," *IEEE Transactions on industrial Electronics*, vol. 62, no. 7, pp. 4355–4364, 2014.
- [8] S. Zuo, A. Davoudi, Y. Song, and F. L. Lewis, "Distributed finite-time voltage and frequency restoration in islanded ac microgrids," *IEEE Transactions on Industrial Electronics*, vol. 63, no. 10, pp. 5988–5997, 2016.
- [9] J. W. Simpson-Porco, F. Dörfler, and F. Bullo, "Voltage stabilization in microgrids via quadratic droop control," *IEEE Transactions on Automatic Control*, vol. 62, no. 3, pp. 1239–1253, 2016.
- [10] M. Arcak, C. Meissen, and A. Packard, Networks of dissipative systems: compositional certification of stability, performance, and safety. Springer, 2016.
- [11] C. De Persis and N. Monshizadeh, "Bregman storage functions for microgrid control," *IEEE Transactions on Automatic Control*, vol. 63, no. 1, pp. 53–68, 2017.
- [12] A. Kwasinski and P. T. Krein, "Stabilization of constant power loads in dc-dc converters using passivity-based control," in *INTELEC 07-*29th International Telecommunications Energy Conference. IEEE, 2007, pp. 867–874.
- [13] J. Schiffer, D. Zonetti, R. Ortega, A. M. Stanković, T. Sezi, and J. Raisch, "A survey on modeling of microgrids—from fundamental physics to phasors and voltage sources," *Automatica*, vol. 74, pp. 135– 150, 2016.
- [14] S. Trip and C. De Persis, "Distributed optimal load frequency control with non-passive dynamics," *IEEE Transactions on Control of Network* Systems, vol. 5, no. 3, pp. 1232–1244, 2017.
- [15] L. Meng, Q. Shafiee, G. F. Trecate, H. Karimi, D. Fulwani, X. Lu, and J. M. Guerrero, "Review on control of dc microgrids and multiple microgrid clusters," *IEEE journal of emerging and selected topics in power electronics*, vol. 5, no. 3, pp. 928–948, 2017.

- [16] Y. Khayat, Q. Shafiee, R. Heydari, M. Naderi, T. Dragičević, J. W. Simpson-Porco, F. Dörfler, M. Fathi, F. Blaabjerg, J. M. Guerrero et al., "On the secondary control architectures of ac microgrids: An overview," *IEEE Transactions on Power Electronics*, vol. 35, no. 6, pp. 6482–6500, 2019.
- [17] M. J. Najafirad and S. Welikala, "Dissipativity-based distributed droop-free control and communication topology co-design for dc microgrids," in 2025 American Control Conference (ACC). IEEE, 2025, pp. 1153–1160.
- [18] S. Welikala, Z. Song, H. Lin, and P. J. Antsaklis, "Decentralized codesign of distributed controllers and communication topologies for vehicular platoons: A dissipativity-based approach," *Automatica*, vol. 174, p. 112118, 2025.
- [19] M. Arcak, "Compositional Design and Verification of Large-Scale Systems Using Dissipativity Theory: Determining Stability and Performance From Subsystem Properties and Interconnection Structures," *IEEE Control Systems Magazine*, vol. 42, no. 2, pp. 51–62, 2022.
- [20] S. Welikala, H. Lin, and P. J. Antsaklis, "Non-linear networked systems analysis and synthesis using dissipativity theory," in 2023 American Control Conference (ACC). IEEE, 2023, pp. 2951–2956.
- [21] —, "On-line estimation of stability and passivity metrics," in 2022 IEEE 61st Conference on Decision and Control (CDC). IEEE, 2022, pp. 267–272.
- [22] P. Nahata and G. Ferrari-Treeate, "Passivity-based voltage and frequency stabilization in ac microgrids," in 2019 18th European Control Conference (ECC). IEEE, 2019, pp. 1890–1895.
- [23] H. S. Khan and A. Y. Memon, "Active and reactive power control of the voltage source inverter in an ac microgrid," *Sustainability*, vol. 15, no. 2, p. 1621, 2023.
- [24] K. Zuo and L. Wu, "An asymptotic stability guaranteed droop-free control scheme for normalized power consensus in microgrids," in 2023 IEEE Power & Energy Society General Meeting (PESGM). IEEE, 2023, pp. 1–5.